Title
Electrical, electromagnetic and structural characteristics of carbon nanotube-polymer nanocomposites

Author
Park, Sung-Hoon

Publication Date
2009

UNIVERSITY OF CALIFORNIA, SAN DIEGO

Electrical, electromagnetic and structural characteristics of Carbon Nanotube-Polymer nanocomposites

A dissertation submitted in partial satisfaction of the
requirements for the degree Doctor of Philosophy
in
Materials Science and Engineering

by

Sung-Hoon Park

Committee in Charge:

Professor Prabhakar R. Bandaru, Chair
Professor Sungho Jin
Professor Vlado A. Lubarda
Professor Vitali F. Nesterenko
Professor Jie Xiang

2009

The dissertation of Sung-Hoon Park is approved, and it is acceptable in quality and form for publication on microfilm and electronically:

Chair

University of California, San Diego

2009

Dedicated

to

My family

Table of Contents

Signature Page……………………………………………………………………..….iii

Dedication Page…………………………………………………………….……iv

Table of Contents………………………………………………………................v

List of Figures…………………………………………………………….…….viii

List of Tables…………………………………………………….…………….…xiv

Acknowledgement……………………………………………….…………..….xv

Curriculum Vita…………………………………………………..…………....xvii

Abstract of the Dissertation……………………………………...……….......xix

Chapter 1. Introduction…………………………………………………...…….1

1.1 Composite filler: Carbon nanotubes (CNTs)…………………………...……….3

1.2 Electrical percolation in nanotube composites……………………………….8

    1.2.1 Electrical percolation threshold…………………………………….………..8

    1.2.2 Prediction of Electrical percolation threshold …………………...…………13

1.3 Composite preparation……………………….…………………………..……….19

    1.3.1 Solution blending process………………………………………….…….19

    1.3.2 Melt blending process………………………………………...……….20

    1.3.3 In Situ polymerization……………………………………………………20

Chapter 2. Electromagnetic interference shielding (EMI) properties of functionalized carbon nanotube composites……………………………….………21

2.1 Introduction…………………………………………………………………….21

2.2 Experimental Procedures………………………………...…………………24

2.3 Results and discussion ……………………………………………………….……..32

2.3.1 DC conductivity and percolation threshold……………………...………32

2.3.2 Shielding effectiveness (SE) of SWNT/RET composites…………….……33

2.3.3 Reflection and absorption of electromagnetic wave in CNT composites…..34

2.3.4 Aspect ratio affect of nanocomposites…………………………….……..37

2.4 Summary……………………………………………………………………….38

Chapter 3. Dielectric properties of functionalized carbon nanotube composites……………………………………………………………………40

3.1 Introduction……………………………………………………….…………40

3.2 Experimental procedures: Dielectric measurement set up…………………..……41

3.3 Results and discussion…………………………………………………..……..43

3.3.1 Real and imaginary permittivity……………………………………..……..44

3.3.2 DC conductivity, AC conductivity and SE……………………….……..46

3.4 Summary……………………………………………………………………….49

Chapter 4. Enhanced mechanical properties of functionalized carbon nanotube composites…………………………………………..……………………..50

4.1 Introduction……………………………………………………...………..50

4.2 Experimental Procedures..…………………………………..………………52

4.3 Results and discussion…………………………………………………………53

4.3.1 Tensile strength and elastic modulus of nanocomposites………………..…53

4.3.2 Toughness and elongation of nanocomposites……………………….…….58

4.4 Summary…………………………………………………………………….62

Chapter 5. Enhanced dielectric constants and electromagnetic shielding in polymer nanocomposites through the use of coiled carbon nanotubes……………………………………………………..……………………63

5.1 Introduction

5.2 Experimental Procedures……………………………………..……………63

5.3 Results and discussion…………………………………………………………65

5.4 Summary…………………………………………………………………….70

Chapter 6. Summary of dissertation……………………………………..………71

References…………………………………………………………………..…74

List of figures

Figure 1-1 Schematic diagram of Electromagnetic Interference (EMI) problem…...…2

Figure 1-2 (a) Single-walled carbon nanotube (b) Multi-walled carbon nanotube (c) Carbon nanotube rope(bundle)………………………...…………………...…4

Figure 1-3 Schematic diagram of oxidation process using sulfuric and nitric acids which yields functionalization of CNT surfaces………………………..….5

Figure 1-4 Schematic attachment of amide group to SWNT………………..………6

Figure 1-5 Schematic diagram of the noncovalent functionalization of bundles of carbon nanotubes (the wrapping of the bundles by the polymer)……………….6

Figure 1-6 Schematic view of two composites (a) spherical shape filler composite (e.g., carbon black) (b) oblong shape filler composite (e.g., carbon fiber, nanotube)……………………………………………………………………...8

Figure 1-7 RF conductivity of (a) Composite with 0.35 wt% carbon nanotubes (b) composite with 50 wt % carbon black. Curves show conductivity from the measurement (solid line) and simulation (dashed line)………………………….9

Figure 1-8 Scanning Electron Microscope (SEM) of fractured cross-section of CNTs/polymer composites: (a) 4 wt% CNTs/PET; (b) 4 wt% CNTs/PE; (c) 8 wt% CNTs/PP; (d) 8 wt% CNTs/varnish…………………………...……….12

Figure 1-9 (a) Two widthless stick (shaded area) and their corresponding excluded area. This area is the parallelogram which is obtained by following the center 0 of the j as it travels around the stick i while being parallel to itself and touching stick i at a single point. (b) Two sticks of length L, width W and radius of caps is W/2. The excluded area is obtained by following the center 0 as stick j travel around stick i while touching it at least at one point. (c) Capped rectangle and the corresponding excluded area which is obtained with θ=0. In three dimensions the stick is a capped cylinder and so is the excluded volume. Both the stick and the excluded volume are obtained by rotating the two dimensional figure around the axis shown……………………………………………….………14

Figure 1-10 The effect of aspect ratio (L/D) on threshold volume fraction for 3D-system: Comparison with references………………………………………..17

Figure 2-1 A high aspect ratio, pertinent to carbon nanotubes, enables very low threshold volume fractions for electrical percolation. The threshold-aspect ratio curve, for uniformly dispersed nanotubes, has been simulated from percolation theory while the ★ indicates results from our experimental measurements……………………………………………………….….…22

Figure 2-2 Schematic diagram of the reaction between functional groups on the CNT with the epoxy groups of the Reactive Ethylene Terpolymer (RET) constituted from (1): polyethylene, (2) methyl-methacrylate, and (3) epoxide functional groups. While (1) and (2) contributes to the mechanical robustness, (3) is used for forming ester linkages to the –COOH groups on the functionalized nanotubes for enhanced bonding and dispersion…………………………...….24

Figure 2-3 Nanotube composite fabrication……………………………………….26

Figure 2-4 Fourier Transform Infrared (FT-IR) Spectrograph of the (i) bare –COOH functionalized SWNT (COOH-SWNT) and the (ii) functionalized single walled CNT-RET (COOH-SWNT/RET) composite. The evidence of esterification, and bonding, between the functionalized nanotubes and the RET is seen in the energy up shift of the 1700 cm^{-1} peak to 1740 cm^{-1} (Ar: Aromatic, S: Symmetric, As: Antisymmetric)…………………………………….………27

Figure 2-5 *Uniform* dispersion of functionalized SWNTs in the RET polymer is indicated, through Scanning Electron Microscope (SEM) micrographs, at both (a) 0.2 volume % and (b) 2.2 volume % filling fractions of the SWNTs. On the other hand, (c) non-functionalized SWNTs dispersed into the RET matrix exhibit clumping…………………………………………………...…..28

Figure 2-6 The electrical conductivity of the *functionalized* SWNT-RET composites follows a power law characteristic of percolation like behavior. The inset shows log-log plot of σ to $(P-P_c)/P_c$. (with a threshold volume fraction, $p_c \sim 0.11\%$ and an exponent of ~ 3.4)……………………………………………………..………32

Figure 2-7 (a) An enhanced shielding effectiveness (SE) has been observed for the chemical functional group reaction enhanced SWNT-RET polymers (COOH-SWNT/RET) compared to non-functionalized SWNT-RET composites (Pristine SWNT/RET), and (b) increases with increased filling fraction of the SWNTs…………………………………………………….…….…………33

Figure 2-8 The total shielding efficiency, SE (Tot), can be decomposed into contributions from reflection, SE (R) and absorption, SE (A), through a consideration of the frequency (*f*) dependence. (a) Reflective losses dominate the total SE for low (~ 0.5 volume %) nanotube filling fractions, while (b) the absorption is more important at larger (~ 4.5 volume %) volume fractions…………………………………………………………….……..…34

Figure 2-9 Schematic diagram for EMI shielding material: Black arrows indicate incident microwave (I). Blue arrows indicate reflected microwave (R). Red arrows indicate transmitted microwave (T). Green arrows indicated absorbed microwave (A)…………………………………………………….……..….35

Figure 2-10 The shielding effectiveness is larger for the single-walled CNTs (SWNTs) compared to the multi-walled CNTs (MWNTs) and illustrates the predominant influence of the aspect ratio (SWNT ~ 880, MWNT ~ 30) in determining the percolation and the SE……………………………………..….….………37

Figure 3-1 Schematic diagram of setup for *S*-parameters measurements…………….42

Figure 3-2 SEM micrographs of **(a)** 0.9 volume % and **(b)** 4.5 volume % *functionalized* SWNT-RET composites, **(c)** 2.2 volume % of *non-functionalized* SWNT-RET composites…….…………………………………………...…43

Figure 3-3 The (a) real - ε', and (b) imaginary - ε'' components of the dielectric constants of functionalized SWNT-RET composites (numbers in % indicate volume fraction of SWNTs), are larger than pristine SWNT (p-SWNT) and functionalized MWNT (f-MWNT)-RET composites…………………………45

Figure 3-4 (a) The DC conductivity, σ_{DC}, of functionalized SWNT-RET composites follows a power law characteristic of percolation like behavior (with a threshold volume fraction, $\phi_c \sim 0.11\%$ and an exponent of ~ 3.4). (b) The AC conductivity, σ_{AC}, of the SWNT-RET composite increases linearly with SWNT volume fraction (ϕ_{CNT}), and frequency, at a particular ϕ_{CNT}. The inset shows the parallel resistor-capacitor combination used to model σ_{AC}. (c) The σ_{AC} can be used as a predictor of the shielding effectiveness (SE) of the nanocomposites (numbers indicate ϕ_{CNT})- data obtained at 12.4 GHz. The polymer matrix reference is indicated by RET……………………………………………..….47

Figure 4-1 Stress-strain curves of functionalized SWNT-RET composites with different loading of nanotubes. Composites with low nanotube loading (below 0.9 vol%) show ductile behavior with high elongation whereas after 0.9 vol% loading composites show stiff behavior with high strength…………….…….52

Figure 4-2 Tensile strength of the functionalized SWNT-RET composites (■) and pristine SWNT-RET composites (●) with different loading of SWNTs……...54

Figure 4-3 Elastic modulus of functionalized SWNTs (█) and MWNT (▲) – RET composites and pristine SWNT-RET (●) composites with different loading of nanotubes. Each experimental data were fitted by the the modified Halpin-Tsai equation……………………………………………………………….…55

Figure 4-4 Schematic diagram for constants p related to the degree of nanotubes aggregation. Depending on nanotubes status such as degree of exfoliation, dispersion and curved shape, p (=b/a) values can be different. A larger p could be indicative of CNT aggregation in the polymer…………………...…….57

Figure 4-5 Toughness of functionalized SWNT-RET composites with different loading of nanotubes……………………………………………………….………58

Figure 4-6 SEM images of functionalized SWNT-RET composites after tensile testing. Nanotube bundles work as bridge (red circle) and were pulled out tightly from the crack of the matrix that is different with figure 1(b) (: freeze fracture image without tension)…………………………………………………….………..59

Figure 4-7 Schematic diagram of nanotube composites depend on nanotube concentration. At low CNTs loading (left top and bottom), toughness and elongation are increased. Whereas, at high CNTs loading (right top and bottom), toughness and elongation are decreased due to excess of covalent bonding between CNTs and polymer chain…………………………………...………..60

Figure 5-1 Scanning Electron Microscope (SEM) images (a) Highly aligned coiled carbon nanotubes (CCNs) with nearly identical diameter and pitch. (b) mixed carbon nanotubes (MCNs : coil + linear carbon nanotubes) (c) 2 wt% of CCN-RET composite having uniform dispersion condition. (d) High resolution image of CCN-RET composite…………………….……...…64

Figure 5-2 The DC conductivity of nanotube composites with same 2 wt% filling. (Filler: MWNT, SWNT, MCN, CCN) ……...…………..…………………….65

Figure 5-3 Real (top) and imaginary (bottom) permittivity of nanotube composites (Filler: MWNT, SWNT, MCN, CCN) (a) Comparison with similar diameter and length. (b) Comparison with similar DC conductivity…...............……….66

Figure 5-4 The σ_{AC} of nanotube composites at 8.2 G Hz (Filler: MWNT, SWNT, MCN, CCN). (a) Comparison with similar diameter and length. (b) Comparison with similar σ_{DC}. Inset image schematically shows σ_{DC} portion and σ_{AC} portion. Arrow indicates each σ_{AC}. Conductivity at 0 Hz means DC conductivity which is much smaller than AC conductivity…………………………………………67

Figure 5-5 Schematic diagram of additional capacitive effect in CCNs……………...68

Figure 5-6 Shielding effectiveness (SE) of nanotube composites (Filler: MWNT, SWNT, MCN, CCN) (a) Comparison with similar diameter and length. (b) Comparison with similar DC conductivity……………………………………………...69

List of tables

Table 1-1 Percolation threshold and critical exponent of CNT/polymer composites. PMMA – poly methyl methacrylate, P3OT – poly3octylthiophene, PU – Polyurethane, PC – polycarbonate, PET – poly ethylene terephthalate, PVA – polyvinylalcohol……………………………………………………………11

Table 4-2 Mechanical and electrical properties of functionalized SWCNT/RET composites…………………………………………………………………..…..61

Acknowledgement

I wish to acknowledge and truly thank my advisor, Professor Prabhakar R. Bandaru, for his strong encouragement, support, inspiration, direction during the course of this research. I wish to express my gratitude to my committee members for their time and helpful discussions: Professor Sungho Jin, Professor Vitali F. Nesterenko, Professor Vlado A. Lubarda and Professor Jie Xiang.

Chapter 2, in full, has been published in “Enhanced electromagnetic interference shielding through the use of functionalized carbon nanotube-reactive polymer composites”, IEEE Transactions on Nanotechnology, TNANO-00013-2009.R1 by S. H. Park, P. Thielemann, P. Asbeck, P. R. Bandaru. Chapter 3, in full, has been published in “Enhanced dielectric constants and shielding effectiveness of uniformly dispersed functionalized carbon nanotube composites”, Applied Physics Letters, 94, 243111 ,2009 by S. H. Park, P. Thielemann, P. Asbeck, P. R. Bandaru. Chapter 4, in full, has been submitted to “Enhanced mechanical properties of polymer functional group hybridized carbon nanotube composites” (2009)
, *Carbon* by S. H. Park, P. R. Bandaru.

I would like to show my gratefulness to Paul Thielemann for his many endeavors and his assistance in the study of electromagnetic properties of nanotube composites and I deeply recognize his profound knowledge on microwave behavior of coiled nanotube composites. I greatly thank Dr. Corey T. Love for his great help in the nanocomposite fabrications and functionalization of nanotubes. I would like to appreciate Professor Peter Asbeck for his help in the microwave measurement set up.

.

Many thanks to those who assist me in various aspects of this work: Professor Vistasp M. Karbhari, Professor Seunghan Oh, Professor M. A. Meyers, Dr. Y. Seki and Steve Pfeifer. I appreciate all the helps from my collaborators from Clemson University: Professor Apparao M. Rao and Keqin Yang.

Special thanks go to Charlotte Lauve for taking care of the administrative burdens for me.

I also wish to thank my many friends and other colleagues who are too numerous to mention all by name.

Sung-Hoon Park

La Jolla, October 2009

Curriculum Vita

Education

2002 B.S., Mechanical Engineering

Chung-Ang University, Korea

2006 M.S., Materials Science and Engineering

University of California San Diego, United States

2009 Ph. D. Materials Science and Engineering

University of California San Diego, United States

JOURNAL PUBLICATIONS:

Sung-Hoon Park, Paul Thielemann, Peter Asbeck, Prabhakar R. Bandaru, "Enhanced dielectric constants and shielding effectiveness of uniformly dispersed functionalized carbon nanotube composites", Applied Physics Letters, 94, 243111 ,2009

Sung-Hoon Park, Paul Thielemann, Peter Asbeck, Prabhakar R. Bandaru, "Enhanced electromagnetic interference shielding through the use of functionalized carbon nanotube-reactive polymer composites", IEEE Transactions on Nanotechnology, TNANO-00013-2009, 2009

Sung-Hoon Park, Prabhakar R. Bandaru, "Enhanced mechanical properties of polymer functional group hybridized carbon nanotube composites" (to be submitted to the *Carbon)*

Sung-Hoon Park, Paul Thielemann, Peter Asbeck, Prabhakar R. Bandaru, "Enhanced dielectric constants and electromagnetic shielding in polymer nanocomposites through the use of nonlinear carbon nanotubes" (to be submitted to the Applied Physics Letters)

Sung-Hoon Park, Prabhakar R. Bandaru, “Optimal design carbon nanotube polymer composites for electromagnetic interference shielding – a review” (In preparation)

Steve Pfeifer, Sung-Hoon Park, Prabhakar R. Bandaru, “Application of the weibull probability distribution to analyze the variability of electrical percolation thresholds in carbon nanotube networks” (to be submitted to the Applied Physics Letters)

ABSTRCT OF THE DISSERTATION

Electrical, electromagnetic and structural characteristics of Carbon Nanotube-Polymer nanocomposites

By

Sung-Hoon Park

Doctor of Philosophy in Materials Science and Engineering

University of California, San Diego, 2009

Professor Prabhakar R. Bandaru, Chair

We report on a new type of carbon nanotube (CNT)-polymer nanocomposite with enhanced electrical, electromagnetic and mechanical properties. Such composites were synthesized through a new methodology for integrating CNTs with polymers, where functional groups on CNTs were made to interact with select polymer groups, e.g., epoxy linkages, enabling uniform dispersion over a very wide range of CNT loading. Such composites, e.g., single-walled CNT- RET (reactive ethylene terpolymer), incorporate good CNT dispersion with low electrical percolation volume fractions (~ 0.1 volume %), yielding outstanding microwave shielding efficiency (SE) of ~ 30 dB for electromagnetic interference (EMI) applications. The SE and dielectric properties were characterized for both single-walled and multi-walled CNTs and were

seen to be much enhanced in the former. The specific roles of absorption and reflection in determining the total SE, as a function of the CNT filling fraction was probed in detail.. It was also seen that CNT-RET composites possess a complex dielectric permittivity twenty times larger than composites composed of pristine single walled CNTs and three hundred times larger than functionalized multi-walled CNT-RET composites. We seek to understand such an enhancement, both in terms of uniform nanotube dispersion and through a parallel resistor-capacitor model. We subsequently show that the AC electrical conductivity is a good predictor of the EMI shielding characteristics of nanocomposites.

It was also seen that homogeneous nanostructure dispersion leads to a concomitant *two-fold* increase in the tensile strength and elastic modulus, *E*. We have then proposed, for the first time, a simple model to explain the variation of *E* with CNT filling fraction, even considering the effects of agglomeration. On the other hand, an initial increase in the toughness was observed at low CNT filling fractions, presumably due to incipient crack bridging of the polymer matrix by the CNTs. From a comparison of the properties of single-walled and multi-walled CNT impregnated composites, we ascribe such effects due to the aspect ratio of the nanostructures.

We have also used, for the first time, novel CNT morphologies incorporating helical nanostructures, which seem to yield even better EMI shielding performance compared to linear nanostructures.

Chapter 1. Introduction

A polymer composite is defined as a material constituted of more than one solid phase having matrix (polymer) properties and filler properties. Through doping with various fillers (metals, ceramics, carbon base fiber and semiconductors), matrix properties such as electrical properties, thermal conductivity, magnetic properties, flame resistance and mechanical properties can be enhanced[1-5]. Along with effective processability and low cost, polymer based composites containing conducting filler[6] are very promising for practical applications, such as structural reinforcement[7], electromagnetic interference shielding[8], electronic packaging[9], radar absorbing material[10], and as high charge storage capacitors[11]. In addition, polymer based composites have low density in comparison with metal based or cement based composites[12]. Furthermore, the advent of nanomaterials (carbon nanotubes- CNTs, nanowires- NW, nanoparticle) offers new possibilities for polymer composite research with a high potential for successful commercial development due to its exceptional properties. However, to realize this nanomaterial as a commercial composite filler, further investigations are needed especially in homogeneous dispersion of the nanomaterial to the polymer matrix.

The main objective of this study is aimed at overcoming extant problems in nanocomposite fabrication and to investigate novel polymer nanocomposites for their electromagnetic interference (EMI) shielding properties, dielectric properties and mechanical properties.

In the context of EMI applications, electromagnetic waves from the environment interfere with sensitive electronic instruments and the human body (Figure 1-1). In addition, high frequency, e.g., RF devices can enhance such electromagnetic pollution. For example, cell phone use has been suspected to be one of the major causes for premature cataract[13]. Consequently, a significant amount of research is being conducted to make efficient EMI shielding materials. For example, for military purposes, such as stealth applications, electromagnetic radiation absorbing materials have been widely investigated to immunize against radar. Recently, polymer composites containing conducting filler such as carbon black[14-18], carbon fiber[14-16, 19], nanowire[20] and carbon nanotubes (CNT)[10, 21, 22] have been extensively investigated as EMI shielding materials due to their lightweight, flexibility, corrosion resistance, and good shielding efficiency.

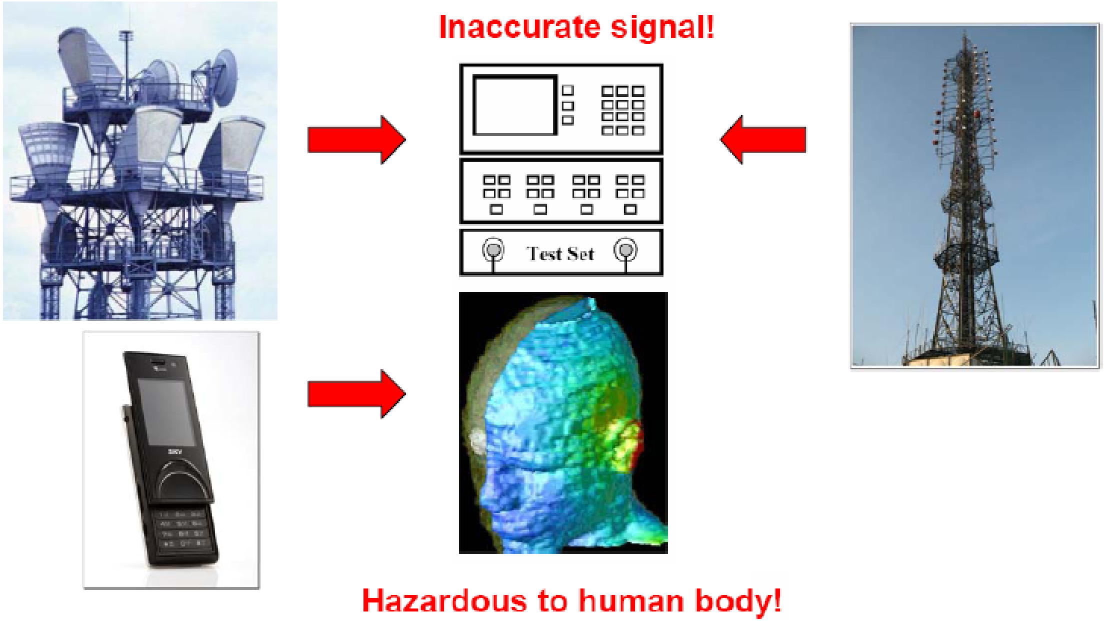

Figure 1-1 Schematic diagram of Electromagnetic Interference (EMI) problem

1.1 Composite filler: Carbon nanotubes (CNTs)

CNTs were proposed as contiguous hollow tubes in the core structure of carbon fibers in 1976[23] (as shown Figure 1-2) with remarkable chemical and physical properties, such as enhanced electrical and thermal conductivity, which makes them ideal candidates for a variety of scientific and technological applications[24-27]. As first observed by Iijima[28], CNTs can be seen as cylinders made from sheets of graphene.

Generally, they are classified in two varieties according to the number of graphite-sheet walls: (a) Single-walled carbon nanotube (SWNT) (b) Multi-walled carbon nanotube (MWNT) as shown Figure 1-2. Depending on the way that the graphene sheet is rolled (arm chair or zigzag structure as shown Figure 1-2 (a)), SWNTs can be metallic or semiconducting. Also, the CNTs are found in the form of carbon nanotube rope (bundles) as shown Figure 1-2 (c).

These quasi-one dimensional molecular systems are typically nanometer-sized in diameter but can be few hundred micrometers in length, yielding a high length to diameter aspect ratio **(**10^2~10^5), high conductivity and small diameter[20, 22, 26, 29, 30]. Moreover, CNTs have huge specific surface area (> 1300 m^2/g for 1 nm diameter SWNTs) which enables various functionalization schemes to be attempted. The large aspect ratio also enables uniform dispersion in a polymer matrix[31] for polymer nanocomposites.

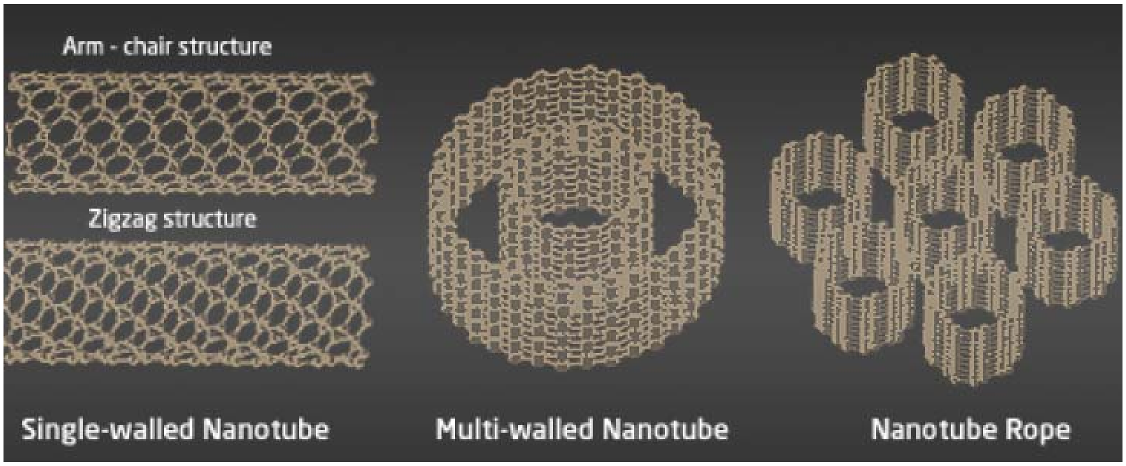

(a) (b) (c)

Figure 1-2 (a) Single-walled carbon nanotube (SWNT) (b) Multi-walled carbon nanotube (MWNT) (c) Carbon nanotube rope (bundle) [32]

However, CNTs, especially SWNTs, with a high aspect ratio often aggregate to form bundles or ropes due to intrinsic van der Waals attractions with an attractive force is ~0.5 eV per nanometer of tube-to-tube contact[33]. Consequently, limited CNT solubility leading to poor dispersion in a polymer matrix results in difficult processing[27, 34]. Aggregations of nanostructures generally imply inhomogeneity leading to an overall deterioration of various properties and also resulting in the use of excess fillers leading to higher cost of the nanocomposite. To exfoliate individual CNTs from bundle type, ultra-sonication and high-shear mixing were used for separating the CNTs, e.g., through first suspending them in organic amide solvents, such as dimethylformamide (DMF) and dichlorobenzene (DCB)[35].

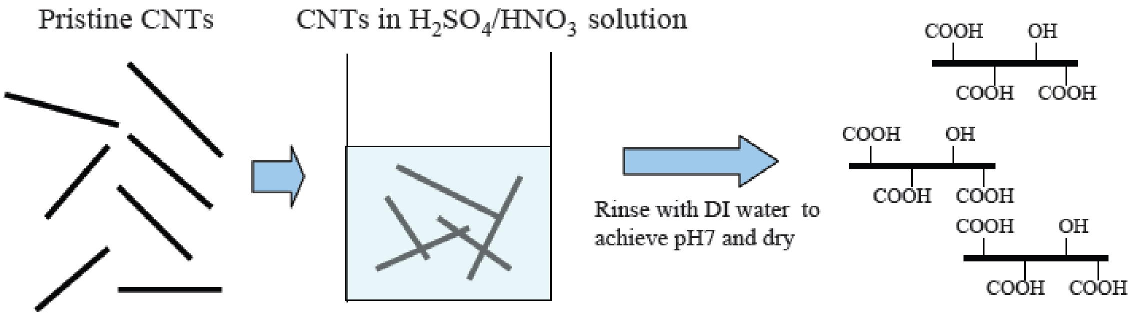

Figure 1-3 Schematic diagram of oxidation process using sulfuric and nitric acids which yields functionalized CNT surfaces

To achieve homogeneous dispersion of CNTs in solvent/polymer matrix, it is often necessary to use chemical functionalization of CNTs to enable reactions with functional groups of the polymer matrix, through a condensation reaction (or esterfication). For this purpose, covalent functionalization can be used to cause disruption of π conjugation on the CNT. Typically, hydroxyl (-OH), carboxyl groups(-COOH), acyl chloride or amide groups, as shown Figure 1-3 and Figure 1-4, can be formed at the defects on the CNT surface, through oxidation or acid treatment of the CNTs[36-38] as schematically shown in figure 1-3, where sulfuric and nitric acids have been used for functionalization.

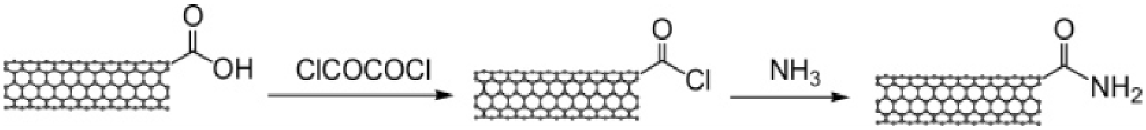

Figure 1-4 Schematic attachment of amide group to SWNT

Generally, the defect-derived carboxylic acids were preferred for functionalization linkages due to well-established reaction schemes and the fact that the nanotube electronic structures are largely preserved post-functionalization[39, 40]. Both acyl chloride and amide groups (as shown in Figure 1-4) are also very reactive with other molecules, so they could be used for covalent bonding with polymer functional groups[41].

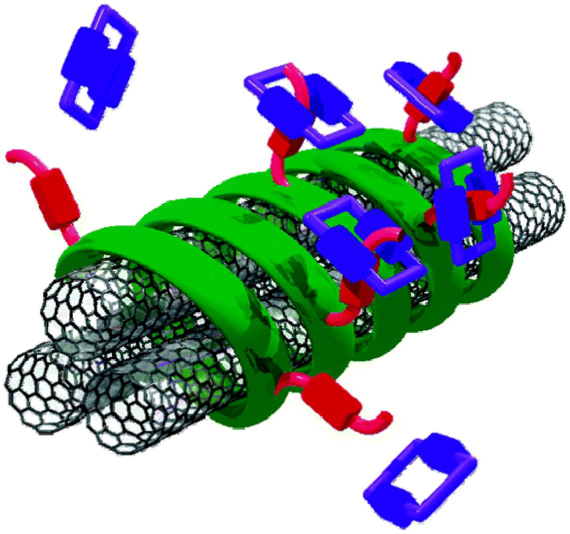

Figure 1-5 Schematic diagram of the noncovalent functionalization of bundles of CNTs (the wrapping of the bundles by the polymer)[42]

Noncovalent functionalization (Figure 1-5) is an alternate method to achieve homogeneous dispersion of CNTs. Using this modification such as polymer wrapping of nanotubes[42], there is no disruption of the sp^2 graphene structure. Consequently, intrinsic CNTs properties can be preserved. However, it often causes weak bonding between nanotube and polymer and poor electrical contact between nanotubes[5, 35].

1.2 Electrical percolation of nanotube composites

1.2.1 Electrical percolation threshold

Electrical percolation threshold is defined as the minimum volume fraction of filler material necessary to form an electrical network in an insulating material (e.g., polymer). Above the critical filler volume fraction, a transition from insulator to conductor like behavior occurs. The percolation threshold is generally dependent on various aspects, such as the intrinsic properties of filler and polymer matrix material, shape and dispersion of filler, etc.

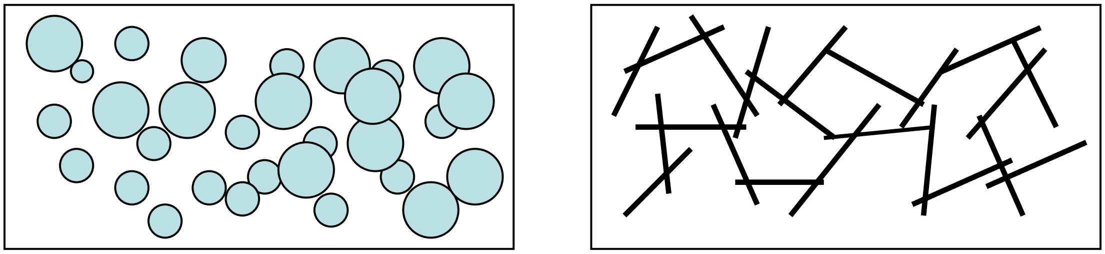

Figure 1-6 Schematic view of two composites (a) spherical shape filler composite (e.g., carbon black) (b) oblong shape filler composite (e.g., carbon fiber, nanotube)

For example, consider two different types of conducting filler in an insulating matrix, one spherical in morphology (e.g., as in carbon black) and the other rod in shape (e.g., carbon fiber), with a large aspect ratio shown Figure 1-6. A higher concentration of the former is needed to form a continuous electrical network, while a smaller concentration of carbon fiber is adequate for creating a conducting network.

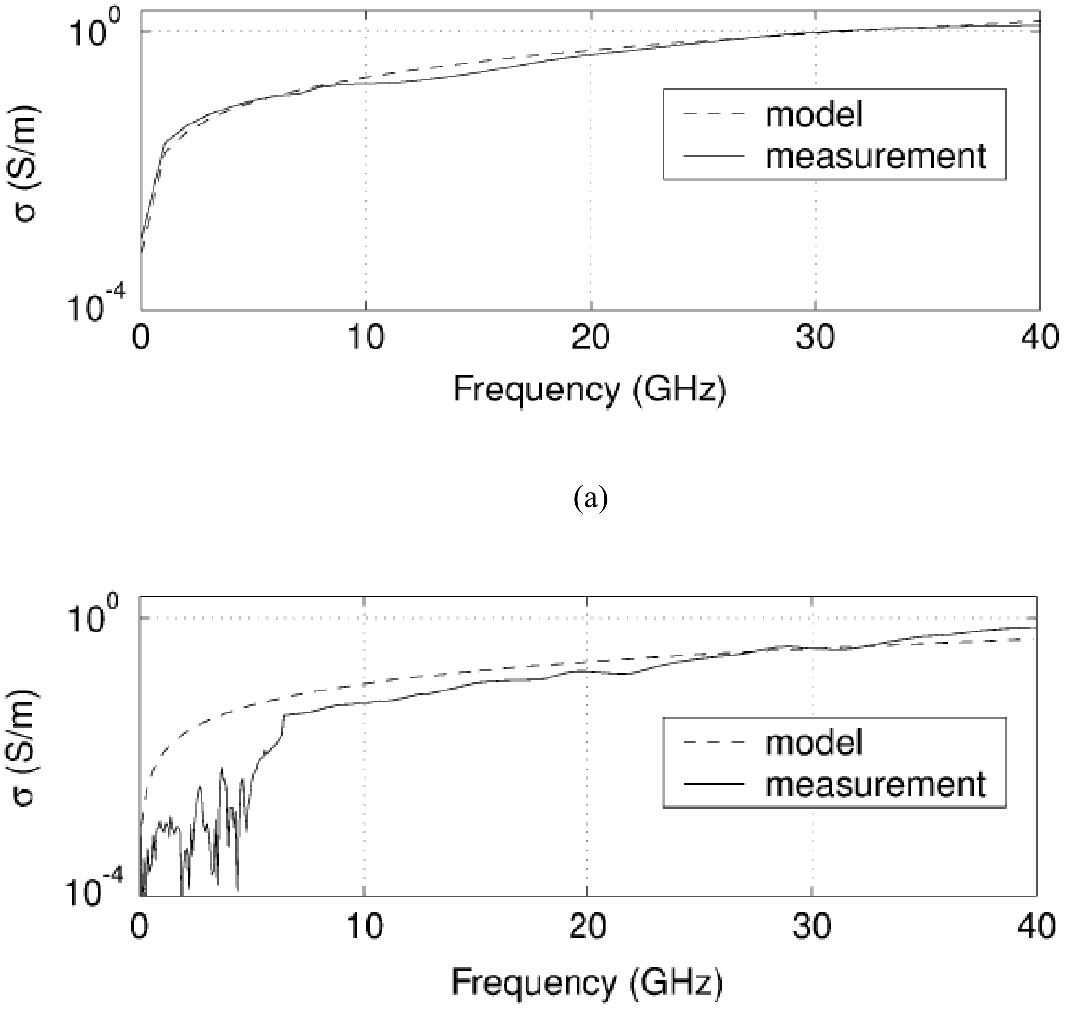

(a)

(b)

Figure 1-7 RF conductivity(σ) of (a) Composite with 0.35 wt% carbon nanotubes (b) composite with 50 wt % carbon black. Curves show σ from the measurement (solid line) and simulation using combination of resistor and capacitor model (dashed line)[43].

Compared with other fillers, CNTs have a large aspect ratio due to their relatively small diameters (~ 1 nm) coupled with their large lengths (1µm – 1 mm) suggesting that only small volume fractions of CNT would be needed to achieve percolation.

Consequently, CNT/polymer composites could be more efficient (in terms of electrical and electromagnetic properties) than conventional powder or particle-filled composites due to extremely high aspect ratio of the nanotubes. For example, to reach conductivity of 1 S/m in composite at the GHz range, it was measured and calculated (using a resistor and capacitor model) that a CNT concentration of only 0.35 wt% (figure 1-7 (a)) was necessary while more than 20 wt% (figure 1-7 (b)) was needed for the carbon black spheres[43].

Generally, the conductivity of composites formed by a conducting filler in a polymer matrix is known to obey a power law given by[44]:

$$\sigma = \sigma_0 (p - p_c)^t \quad \text{for } p > p_c \qquad (1)$$

where σ_0 is the conductivity of an element of a network, p is the concentration, p_c is the percolation threshold, and t is the critical exponent of conductivity(theoretical value of t =1.33 for 2D lattice and $t \approx 1.94$ in 3D)[45, 46]. A small compilation of the observed values of p_c and t values in CNT/polymer composites is tabulated in Table 1-1[10, 22, 46-52].

Table 1-1 shows that even if similar preparation methods, composite electrical percolation thresholds are different. Generally, depending on the polymer type (molecular weight, radius of gyration and its functional group) and intrinsic properties of CNTs, the percolation threshold could be different. For example, by choosing different polymer matrices with same filler (MWNTs) and employing the same fabrication process, the dispersion of CNTs could be quite different (as shown Figure

1-8)[53]. Figure 1-8 shows better dispersion of MWNTs in the polymer matrix at CNT/ Polyethylene terephthalate (PET) and CNT/varnish than the Polyethylene (PE) and Polypropylene (PP) cases. These differences can be explained by the varied efficiency of the efficient reaction between the CNTs and polymer matrix.

Table 1-1 Percolation threshold and critical exponent of CNT/polymer composites. PMMA – poly methyl methacrylate, P3OT – poly3octylthiophene, PU – Polyurethane, PC – polycarbonate, PET – poly ethylene terephthalate, PVA – polyvinylalcohol

Composite	Preparation method	Percolation Threshold (p_c)	Critical exponent (t)	Ref
SWNT/PMMA	Solution mixing	0.39 wt %	2.3	[47]
SWNT/PMMA	Solution mixing	0.17 wt%	2.2	[48]
SWNT/P3OT	Solution mixing	4 wt %	2	[49]
SWNT/PU	Solution mixing	3.4 wt%	4.7	[10]
SWNT/Epoxy	In situ	0.062 wt%	2.68	[22]
SWNT/Epoxy	In situ	0.074 wt%	1.3	[50]
MWNT/PC	Solution mixing	1.44 wt%	2.1	[51]
MWNT/PET	Solution mixing	0.9 wt%	2.2	[52]
MWNT/PVA	Solution mixing	0.055 wt%	1.36	[46]

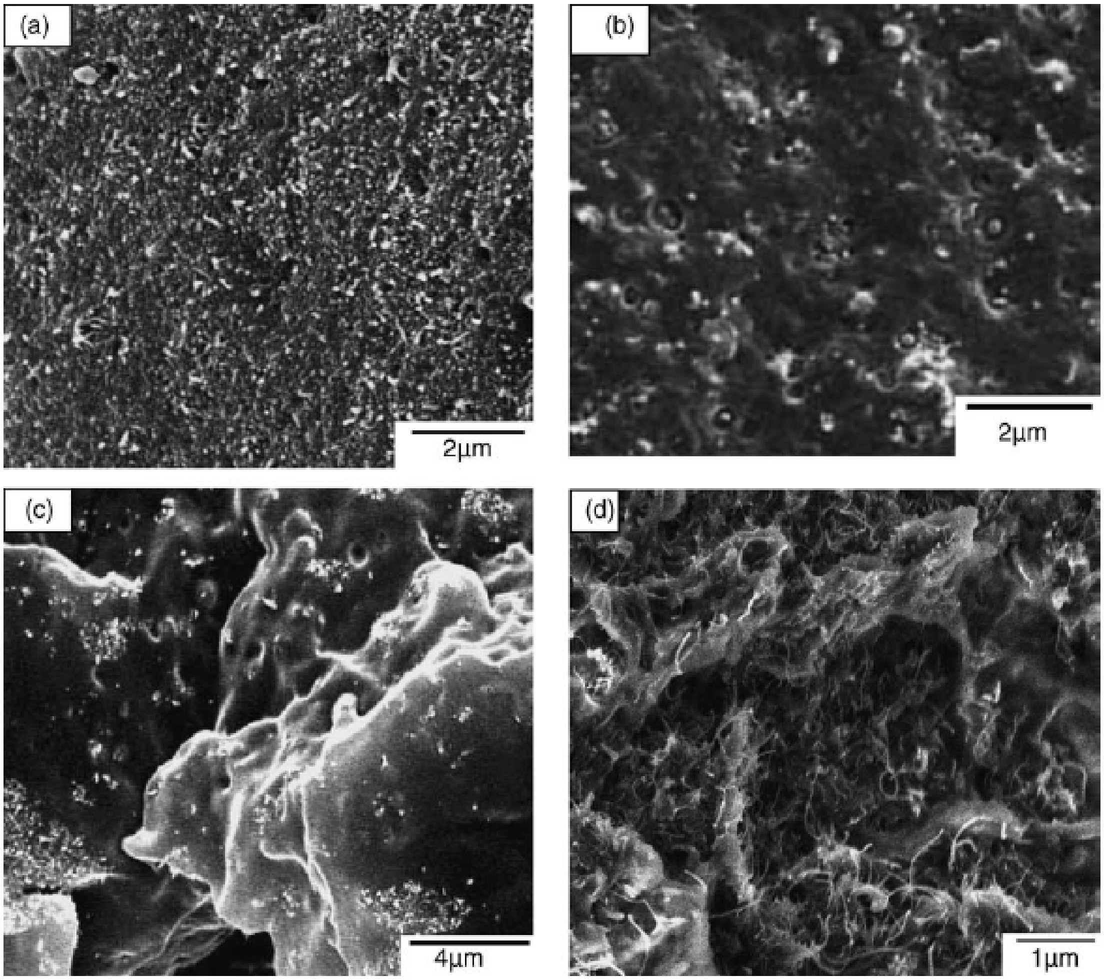

Figure 1-8 SEM of fractured cross-section of CNTs/polymer composites: (a) 4 wt% CNTs/PET; (b) 4 wt% CNTs/PE; (c) 8 wt% CNTs/PP; (d) 8 wt% CNTs/varnish[53]

Functional groups of the polymer that could react with defects on the nanotube surfaces or surface functional groups of nanotube contribute to better dispersion of nanotubes in the polymer matrix. Consequently, efficient dispersion condition increases electrical networking of fillers in polymer matrix leading to the enhancement of overall composite conductivity. For example, CNTs in CNT/PE composite as shown Figure 1-8(b) generally formed clusters while CNTs in CNT/PET composites as shown figure 1-8(a) are relatively well dispersed leading to many more contact boundaries between the polymer and the nanotubes.

1.2.2 Prediction of Electrical percolation threshold

Generally, the electrical properties of the filler/polymer composite depend very sensitively on the dimension and distribution of filler. In earlier work, Pike and Seager[54] proposed a fiber percolation model (FPM) that could predict a threshold fiber volume fraction at which insulating polymer become electrically conductive through the addition of conducting fiber. Taya and Ueda[55-57] have extended this model to the case of two and three dimensionally misoriented short fiber constituted composites, where the threshold fiber volume fraction strongly depends on the aspect ratio of filler and the degree of filler misorientation.

As mentioned earlier, only a small volume fraction of CNTs is necessary to achieve electrical conductivity percolation. This criterion is critical due to the high cost of CNTs. Reliable criteria which predict minimum volume fraction for electrical percolation are addressed next using an excluded volume (or area) based method[58]. In this context, the excluded volume (/area) is defined as the volume (/area) around an object into which the center of another object is not allowed to enter if overlapping of two objects is to be avoided[58-61].

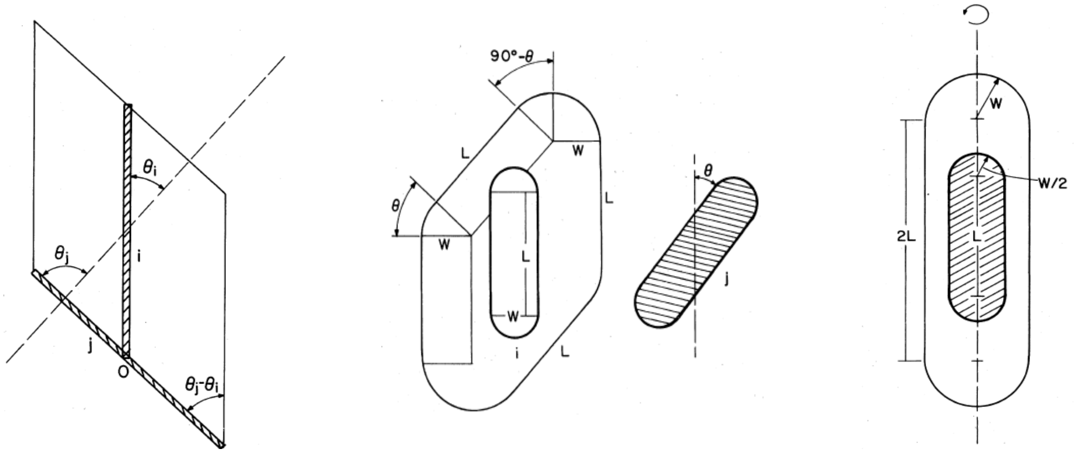

(a) (b) (c)

Figure 1-9 (a) Two widthless sticks (shaded area) and their corresponding excluded area. This area is the parallelogram which is obtained by following the center 0 of the *j* as it travels around the stick *i* while being parallel to itself and touching stick *i* at a single point. (b) Two sticks of length L, width W and radius of caps is $W/2$. The excluded area is obtained by following the center 0 as stick *j* travel around stick *i* while touching it at least at one point. (c) Capped rectangle and the corresponding excluded area which is obtained with $\theta=0$. In three dimensions the stick is a capped cylinder and so is the excluded volume. Both the stick and the excluded volume are obtained by rotating the two dimensional figure around the axis shown[58].

For an elongated object, the excluded volume (/area) could be very different in shape from the actual object and the orientation of the objects[62]. The total excluded volume $[V_{ex}]$ is defined by multiplying this statistically averaged excluded volume $[V]$ by N_c, where N_c is the critical number density of objects in given volume, which are randomly distributed in a unit cube (square). Therefore, the total excluded volume $[V_{ex}]$ is given by

$$[V_{ex}] = [V]N_c. \tag{1}$$

Correspondingly, the total excluded area $[A_{ex}]$ is given by

$$[A_{ex}]= [A]N_c. \tag{2}$$

Firstly, for excluded area of the widthless stick case as shown Figure 1-9 (a), the excluded area is the area of the parallelogram (= $L^2 sin(\theta_i\text{-}\theta_j)$). Where L is a stick of length, θ_i is angle of stick i with respect to a given direction in the plane and θ_j is angle of stick j with respect to same given direction. An ensemble average over all possible orientations of the sticks is considered through evaluating the distribution function of the angles $P(\theta_i)$. The angles between the sticks and a predetermined direction are considered to be randomly distributed within the interval [63]

$$-\theta_\mu \le \theta_i - \theta_j \le \theta_\mu \tag{3}$$

where $\theta_\mu \le \pi/2$, isotropic case $\theta_\mu = \pi/2$ and the smaller the θ_μ, the more anisotropic the system. By considering all possible angles θ_i and θ_j, their corresponding uniform probability is given by[63]

$$P(\theta_i)=1/2\theta_\mu. \tag{4}$$

Therefore, the averaged excluded area is

$$[A] = L^2 \int_{-\pi/2}^{\pi/2} \int_{-\pi/2}^{\pi/2} \sin\left|\theta_i - \theta_j\right| P(\theta_i) P(\theta_j) \times d\theta_i d\theta_j . \tag{5}$$

Substituting equation (4) into (5), we have

$$[A]=\left(L/2\theta_{\mu}\right)^{2}\left[4\theta_{\mu}-2\sin\left(2\theta_{\mu}\right)\right]. \qquad (6)$$

For the isotropic case, the excluded area is

$$[A]=\left(2/\pi\right)L^{2}. \qquad (7)$$

In another example, we consider the excluded area of a capped stick with a finite width as shown figure 1-9 (b) represented through a rectangle of length L, width W and caps of radius $W/2$ at its ends. If the angle between two sticks is $\theta = \theta_i - \theta_j$, the excluded area is obtained by moving one stick around the other stationary stick (shaded area) and registering the center of the moving stick. A calculated excluded area is $4WL+\pi W^2+L^2 sin\theta$.

Therefore, the average excluded area for the case of uniform random orientation distribution, using equations (4) and (5), is given by

$$[A] = 4WL + \pi W^2 + (L/2\theta_\mu)^2[4\theta_\mu-2sin(2\theta_\mu)]. \qquad (8)$$

Excluded volume for two elongated objects as shown figure 1-9 (c) can be found in a similar way through using spherical coordinates θ_i, θ_j, ϕ_j, and ϕ_j. If the angle between the axes of the two capped cylindrical sticks is γ in three dimensions, the excluded volume is $(4\pi/3)W^3+2\pi W^2+2WL^2(sin\gamma)$.

Therefore, averaged excluded volume of the randomly oriented system is

$$[V] = (4\pi/3)W^3 + 2\pi W^2L + 2WL^2 [sin\gamma]_\mu \qquad (9)$$

where $[sin\gamma]_\mu$ is the average value when θ_i and θ_j are confined to an angle of $2\theta_\mu$ around the z axis of the system. For isotropic and perfectly aligned case, value of $[sin\gamma]_\mu$ has been determined to be[58, 62]

$[sin\gamma]_\mu = 0.78 \approx \pi/4$ (for isotropic case) and $[sin\gamma]_\mu = 0$ (for perfectly aligned case).

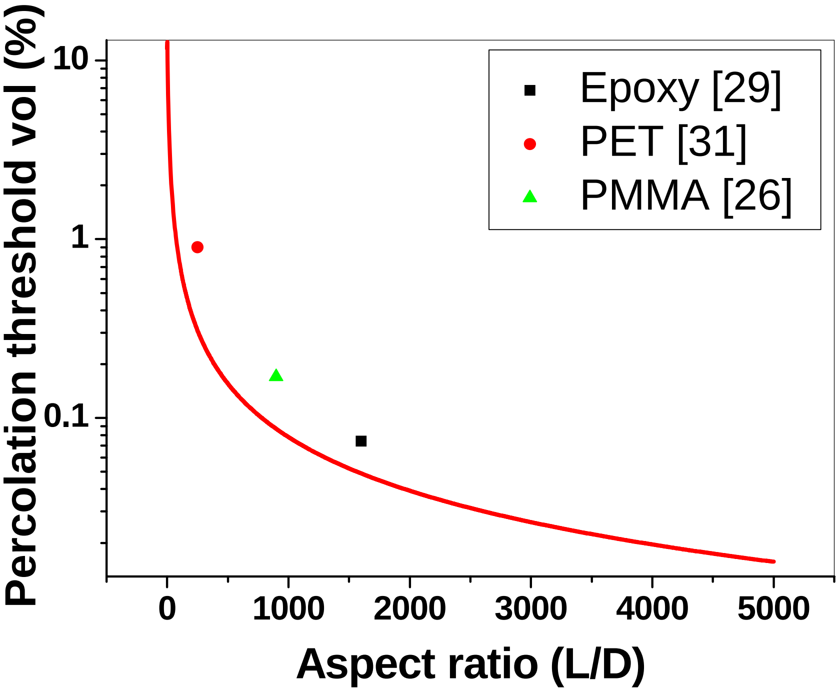

Figure 1-10 The effect of aspect ratio (L/D) on threshold volume fraction for a 3D-system: Comparison with reference[48, 50, 52].

The percolation volume fraction of a 3D fiber system is associated with total excluded volume. In a 3D system, the percolation (critical) volume fraction ($p_c = \phi_c$) is defined as[61],

$$\phi_c = 1 - \exp\left(-N_c v\right) \tag{10}$$

where v is volume of each nanotube. From equation (1), we get

$$\phi_c = 1 - \exp\left(-\frac{\left[V_{ex}\right]v}{\left[V\right]}\right) \tag{11}$$

where the total excluded volume $[V_{ex}]$ was found to be 1.41 for 3D elongated sticks[58, 64].

Therefore, from equations (9) and (11), it can be derived that

$$\phi_c = 1 - \exp\left(-\frac{\left[V_{ex}\right]\left[\left(\pi/4\right)D^2L + \left(\pi/6\right)D^3\right]}{\left(4\pi/3\right)D^3 + 2\pi D^2 L + 2DL^2\left[\sin\theta\right]_{\mu}}\right) \tag{12}$$

Based on equation (12) and assuming randomly oriented isotropic distribution for the CNTs, the relation between the p_c $(= \phi_c)$ and aspect ratio (L/D) of CNTs (modeled as elongated sticks) is shown Figure 1-10. In the figure, some experimental data from Table 1 seems to be well matched to the theoretical curve, suggesting efficient and well dispersed fabrication[48, 50, 52]. The figure could also be used to illustrate, for example, that higher p_c values compared to the curve imply smaller CNT contributions, e.g., aggregation or bundling of the CNTs in the polymer matrix[63].

1.3 Composite preparation

To implement CNT as commercial filler in composite materials, efficient processing is crucial. From Table 1-1 and various studies, the electrical properties of nanocomposite such as percolation threshold are different and inconsistent due to several factors. The dispersion of pristine nanotubes in the polymer by itself is insufficient to achieve uniform results. Therefore, optimal and efficient fabrication is needed to reduce variation of composite properties. The primary goal of current fabrication of CNT/polymer composite for electrical applications is to improve CNTs dispersion in the polymer matrix. The most general fabrication processes of polymer composites are described below, and include our own.

1.3.1 Solution blending process

This is a common method to fabricate polymer matrix carbon nanotube composites due to its simplicity and effectiveness for small size samples[35, 65, 66]. It consists of four steps: 1) disperse the nanotubes in suitable solvent 2) dissolve the polymer in the same solvent 3) mix nanotubes with polymer in solution 4) recover the composite film after evaporating the solvent. Due to intrinsic van der Waals attraction between CNTs, it is difficult to disperse the pristine CNTs in a polymer matrix. Ultra-sonic agitation and functionalization of nanotube surface leading to efficient reaction with functional groups of the polymer will help in their uniform dispersion.

However, during slow solvent evaporation, CNTs tend to agglomerate[67]. Dropping the CNT/polymer suspension on a hot substrate[68] can reduce evaporation time. In addition, coagulation method[69] may prevent agglomeration of the CNTs during evaporation by pouring a CNT/polymer suspension. Our CNTs composite also used such a solution blending process and the detailed processing steps will be described later.

1.3.2 Melt blending process:

Melt blending process is suitable for insoluble Polymers and thermoplastic polymers (by adding CNTs to the polymer melts). This method is compatible with current industrial practice and uses high temperatures coupled with shear force application to disperse CNTs in polymer matrix. However, melt blending is limited to lower concentration and is less effective for dispersing CNTs compared with the previous solution method due to the high viscosities of the composites at higher nanotube loading[35, 67, 70, 71]. Successful examples of the melt process are MWNT/nylon-6[72], SWNT(MWNT)/polycarbonate[73], SWNT/polypropylene[74] and SWNT/polyimide[75] type nanocomposites.

1.3.3 In Situ Polymerization

This method is suitable for insoluble and thermally unstable polymers. CNTs are dispersed in monomer followed by polymerizing the monomer. At this time, polymerization occurs on the surface of CNTs. Using various chemical reactions, the macromolecules of polymer are conjugated to CNTs that enable covalent boding between CNTs and polymer. Usually, CNT/epoxy composites are fabricated by this method where the CNTs are initially dispersed in the epoxy resin followed by curing with a hardener[76, 77]. The extent of in situ polymerization reactions can be limited by increasing the viscosity of reaction medium.[35]

Chapter 2. Electromagnetic interference shielding (EMI) properties of functionalized carbon nanotube composites

2.1 Introduction

The advent of carbon nanotubes (CNTs) and recent studies in polymer-CNT composites[78] has motivated study of their use for Electromagnetic Interference (EMI) applications as light-weight, high shielding efficiency materials. At the very outset, in EMI shielding, the effects of both reflection and absorption of the incident EM radiation have to be considered[79]. The intensity of the reflected radiation (R) is related to the difference of the characteristic impedances (Z) of the incident medium (i.e., air of impedance Z_a) and the material (Z_m) through $R = (\frac{Z_a - Z_m}{Z_a + Z_m})^2$. The absorption (A) is quantified through the skin depth (δ), the extent to which the radiation, of frequency *f*, penetrates the material, through $\delta = \sqrt{\frac{1}{\pi f \mu \sigma}}$, where μ is the magnetic permeability and σ the electrical conductivity. Consequently, while metallic materials (with low Z_m and high σ) are obviously efficient shielding materials, issues such as cost and bulk preclude their wide scale application. Such issues have encouraged the use of polymers where the intrinsic poor conductivity could be compensated through the use of filler materials which form a conducting network. (It is to be noted that electrically conducting polymers are currently expensive, difficult to process, and need considerable improvement in their mechanical properties[80]).

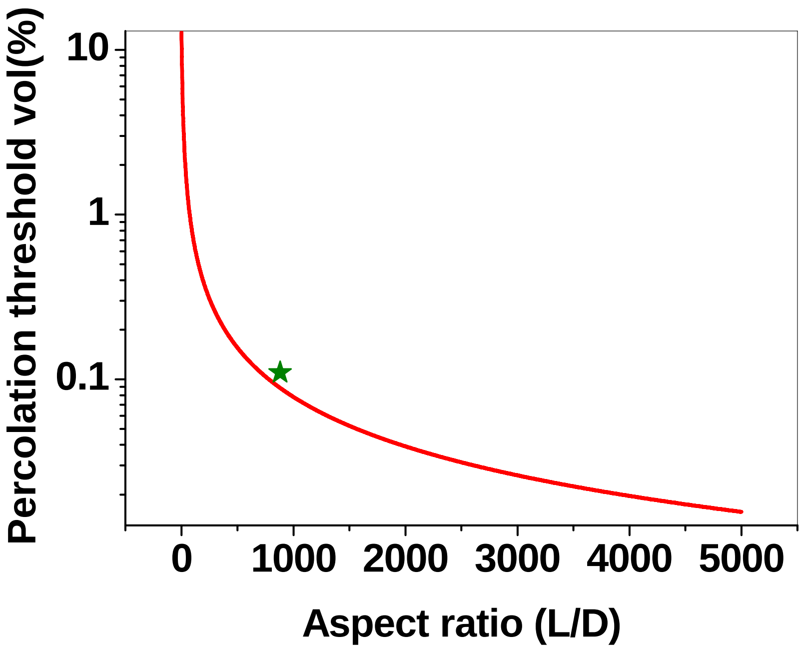

Figure 2-1 A high aspect ratio, pertinent to carbon nanotubes, enables very low threshold volume fractions for electrical percolation. The threshold-aspect ratio curve, for uniformly dispersed nanotubes, has been simulated from percolation theory while the ★ indicates results from our experimental measurements.

While carbon based materials, such as carbon black and fibers, have previously been used in polymer composites[81], their widespread use is limited due to a maximum loading capability, beyond which there is embrittlement. CNTs then, are more attractive candidates for filler materials in composites, primarily due to their large aspect ratio and tunable electrical conductivity, which enables electrical percolation to be achieved with *very small* amounts of nanotubes. For example, we have calculated from the excluded-volume percolation theory of rod-like systems [58, 82, 83] (Figure 2-1) that single walled CNTs (SWNTs) with an aspect ratio of ~ 5000 (which corresponds to a length of 5 µm and a diameter of ~ 1 nm), when dispersed uniformly into a non-conducting polymer enable a conducting pathway at a volume fraction of ~ 0.01 %. Our results on SWNT-RET polymers, which we report in this paper, yield values very close to the optimal considerations (as indicated by the ★ in Figure 2-1).

In our experiments, we have also observed higher values of the electromagnetic interference (EMI) shielding efficiency (SE) at a lower loading fraction of SWNTs (i.e., ~ 30 dB at 4.5 vol % of functionalized SWNTs) compared with literature. A few examples of the SE values from literature include: (i) < 17 dB with 15 vol % SWNTs in SWNT/epoxy composites[84, 85] (ii) < 20 dB with 11.6 vol % SWNTs in SWNT/polyurethane composites at 8 GHz[86], (iii) ~ 20 dB with 8 vol % SWNTs in SWNT/vinyl acetate based composites at 8 GHz[87]. The superior performance of our particular composites could presumably be due to the uniformity of dispersion obtained through functionalization along with a larger aspect ratio. Additionally, our values are comparable to those obtained in CNT films, of ~ 28 dB at 10 GHz[88].

2.2 Experimental Procedures

For large scale processing, it is desirable[78] to ensure effective *mixing* and dispersion of the CNTs within the polymer. The consequent enhanced nanotube-polymer interactions, which are obtained, for example, through chemical functionalization, enable low critical volumes for electrical percolation. In this paper, we tackle such issues in detail and also consider the relative influences of both single walled and multi-walled carbon nanotubes in terms of their shielding efficiency.

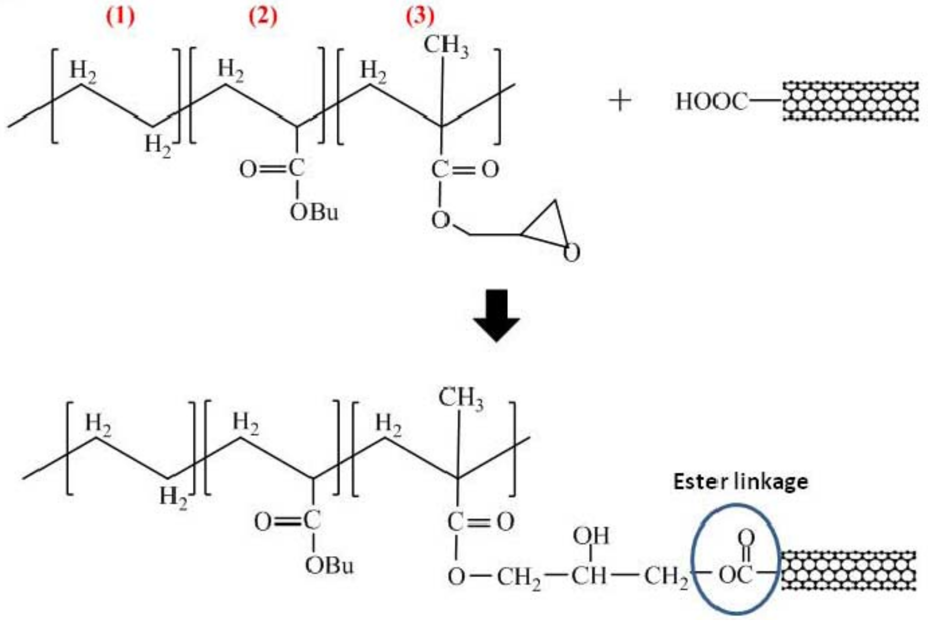

Figure 2-2 Schematic diagram of the reaction between functional groups on the CNT with the epoxy groups of the Reactive Ethylene Terpolymer (RET) constituted from (1): polyethylene, (2) methyl-methacrylate, and (3) epoxide functional groups. While (1) and (2) contributes to the mechanical robustness, (3) is used for forming ester linkages to the –COOH groups on the functionalized nanotubes for enhanced bonding and dispersion.

We chose for our experiments, a composite of CNTs and a Reactive Ethylene Terpolymer (RET: Elvaloy 4170, density 0.94g cm^{-3}) constituted from (1) polyethylene, (2) a polar methyl-methacrylate group, and (3) epoxide functional groups – Figure 2-2. While (1) and (2) contribute to the mechanical characteristics (elastomeric properties) and corrosion resistance underlying the utility of RET as a hot-melt adhesive and coating, the epoxy group has high reactivity[89] and is amenable for effective anchoring of the ring bonds with functional groups(e.g. -OH, COOH, $-NH_2$ etc.) on the carbon nanotubes. The underlying rationale then, is that the epoxide ring rupture [90] on the RET would be facilitated by the –COOH groups on the functionalized nanotubes (Figure 2-2) and then contribute to bonding between the COOH on the SWNT with the epoxy group of the RET.

We used both pristine and carboxyl functionalized SWNTs (average diameter 1-2 nm, length 5-20 μm, 90% purity, and density 2.1g cm^{-3}) and multi-walled carbon nanotubes (MWNTs, average diameter 140 nm, length 5-9 μm, 90% purity, and density 1.7g cm^{-3}) were used. A mixture of sulfuric and nitric acids (in a 3:1 ratio) was used both for nanotube surface functionalization, with –COOH groups, and for removing impurities[89]. Subsequently, the nanotubes were rinsed with deionized water, and then dried at 60 ^{o}C for 10 hours. The MWNTs and SWNTs were then dispersed in toluene with sonication for 20 minutes. (It was typically seen, through Atomic Force Microscopy (AFM) characterization that the above procedure, including sonication, reduces the average length of the SWNTs to ~ 4.3 μm, with a bundle diameter ~4.8 nm, resulting in an aspect ratio of ~ 880. On the other hand, the MWNT an average length of 5.6 μm, with a bundle diameter ~190 nm, yielding an aspect ratio of ~ 30). The RET was then added to toluene solvent with heating, to ~ 60 °C for 2 hours, and subsequent stirring. The nanotube dispersion was then added to the RET solution and sonicated again for ~ 50 minutes. To remove excess solvent, the mixture was stirred, at 60 °C for 3 hours, and poured into glass dishes, and evacuated in vacuum (10^{-3} Torr) for 12 hours. Subsequently, a hot press was used to press the composites into desired thickness. Detail fabrication steps are shown figure 2-3.

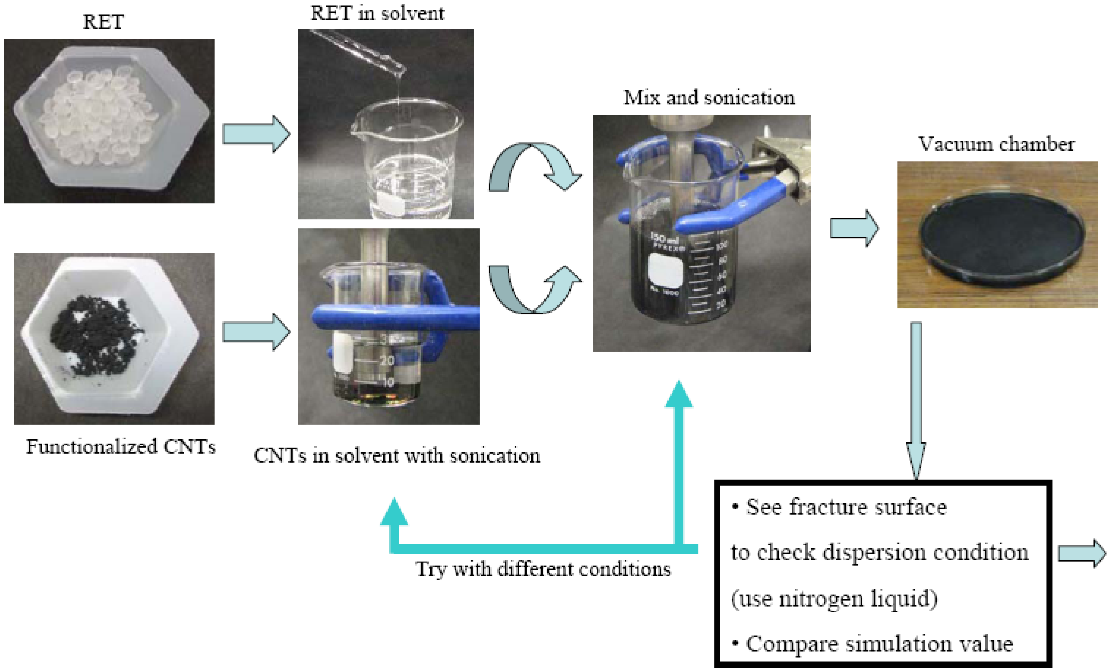

Figure 2-3 Nanotube composite fabrication

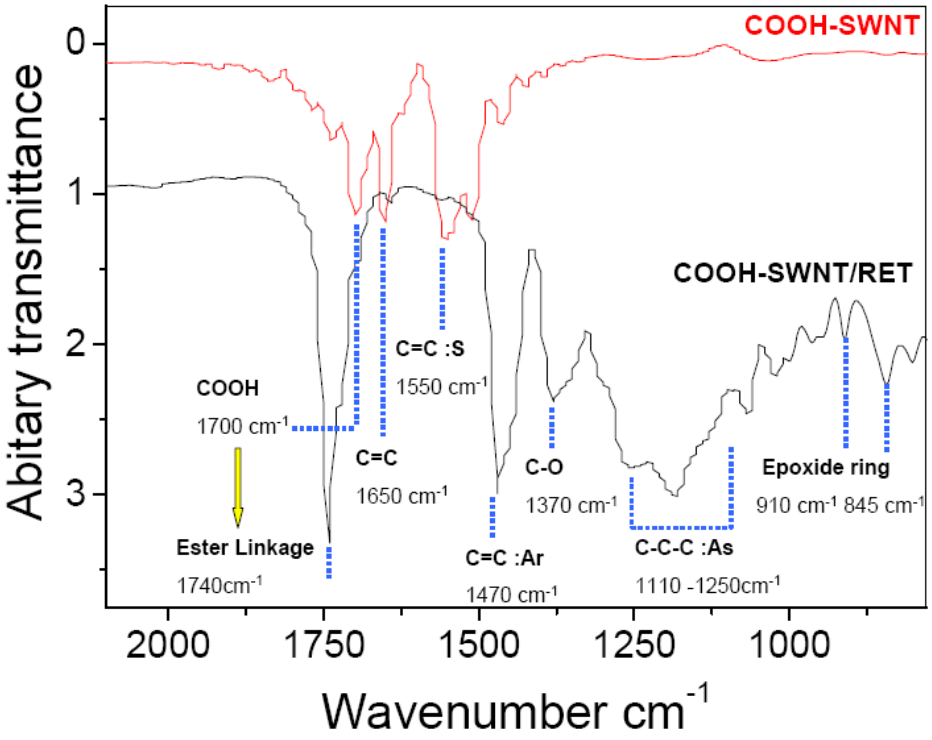

Figure 2-4 Fourier Transform Infrared (FT-IR) Spectrograph of the (i) bare –COOH functionalized SWNT (COOH-SWNT) and the (ii) functionalized single walled CNT-RET (COOH-SWNT/RET) composite. The evidence of esterification, and bonding, between the functionalized nanotubes and the RET is seen in the energy up shift of the 1700 cm^{-1} peak to 1740 cm^{-1} (Ar: Aromatic, S: Symmetric, As: Antisymmetric)

Fourier Transform Infrared (FT-IR) Spectroscopy (Nicolet Magna-IRTM Spectrometer 550) was used to provide proof of covalent bonding [91] between the nanotubes and the RET, and was evidenced by the energy up-shift of the C=O stretch (at 1700 cm^{-1}) - due to the carboxyl group of the –COOH functionalized SWNT – to 1740 cm^{-1} due to the bonding/formation of an ester linkage (Figure 2-4).

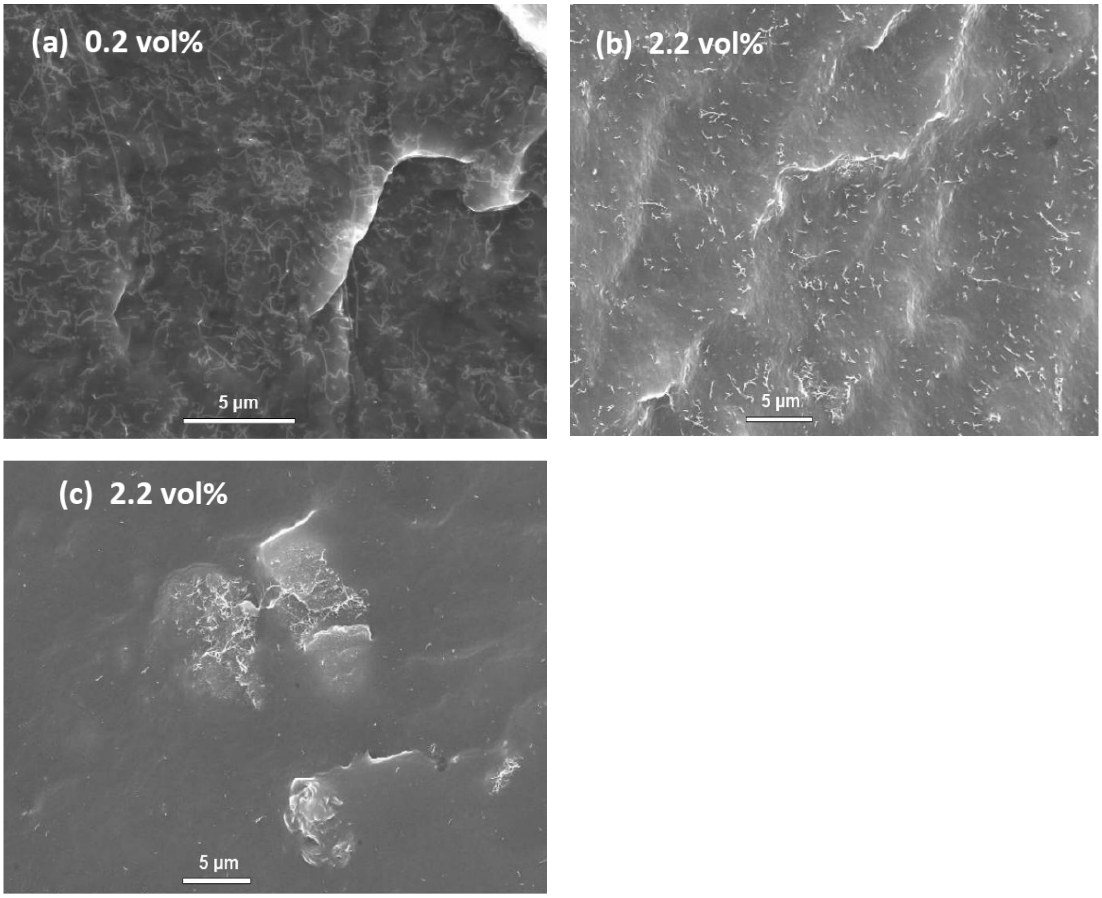

Figure 2-5 *Uniform* dispersion of functionalized SWNTs in the RET polymer is indicated, through Scanning Electron Microscope (SEM) micrographs, at both (a) 0.2 volume % and (b) 2.2 volume % filling fractions of the SWNTs. On the other hand, (c) non-functionalized SWNTs dispersed into the RET matrix exhibit clumping.

The exact location of the functional groups would depend on the defect density on the nanotubes which can be manipulated[92]. However, if the defects are considered to be randomly dispersed, isotropic bonding of the nanotubes with the polymer matrix is implied and could yield uniform dispersion and mixing. While different strategies have been used for homogeneous dispersion[93, 94], it has been generally observed that covalent stabilization [95] and intimate chemical reaction[91, 96] could be beneficial for enhanced electrical conductivity and electromagnetic shielding effectiveness.

In line with the above reasoning, we have indeed observed a more uniform dispersion using functionalized SWNTs for both low (Figure 2-5(a)) and high (Figure 2-5(b)) nanotube filling fractions, as seen in the Scanning Electron Microscopy (SEM: Phillips XL30) images of the fracture surfaces of the CNT/RET composite. The beneficial effects of our proposed scheme of functionalization are also evident through a more homogeneous dispersion of the CNTs in the polymer matrix in comparison to the clumping observed (Figure 2-5(c)) when un-functionalized/pristine nanotubes are mixed into the polymer. (Note that a more rigorous quantification of uniform dispersion is challenging due to the different length scales involved[97]). A thickness of ~ 2 mm of the CNT-RET polymer composite was used for all the measurements reported in this paper. The four-wire resistance method was used to measure the resistance (R) for composites with R < 1G Ω, using the Keithley 487 picoammeter and the Keithley 2400 Sourcemeter. For the resistance measurements, we used samples with rectangular cross-section (5 mm wide X 2 mm thick, typically). The outer current leads were separated by 25 mm while the inner voltage leads were separated by 15 mm. For higher resistance (> 1G Ω) composites, two point measurements using the Agilent B1500A semiconductor device analyzer, with triaxial probes were used. In both cases, the composites were treated with oxygen plasma (Oxford Plasmalab 80 RIE**)** prior to electrical contacting of the surface. Subsequently, 50nm of gold were sputtered on for making electrical contacts. We next monitored the EMI shielding effectiveness (SE) of the synthesized composite in the microwave frequency range (8.2-12.4 GHz: X-band) using a two-port vector network analyzer (Agilent 5242A PNA-X). The X-band is used for both civil and military communications with applications as diverse as weather monitoring, vehicular detection and air traffic control and defense tracking[98]. The desired amount of conducting filler is dependent on the required shielding effectiveness (SE), where $SE = 10\log\frac{p_i}{P_t}$, where P_i and P_t are the magnitudes of the incident and transmitted power densities and were measured through the network analyzer. The initial calibration was performed using the TRL (Thru-Reflect-Line) method [99] which is an improvement over the traditional OSL (Open-Short-Load) calibration technique. In the TRL calibration, the “Thru” measurement was first performed by connecting the two 15 cm waveguide sections directly and measures the total loss and phase delay of the setup, in the absence of the sample. For the “Reflect” calibration, an aluminum short/load was placed between the waveguide sections, while the “Line” calibration was done through the insertion of a quarter-wave section of waveguide (WR-90). These latter measurements serve to accurately delineate the plane of the DUT (device under test) through a consideration of the reflections and other losses prevalent in the test setup including the cabling, waveguide segments and transitions, without the sample. The scattering parameters obtained from the calibration were then used for the baseline.

The CNT-polymer composite was pressed into a sample holder of size 0.9” X 0.4” - standard size for the X-band frequency range. The composite loaded sample holder was then inserted between two 15 cm lengths of WR-90 X-band waveguide to mitigate the near-field effects of the coax to waveguide transitions used to connect the structure to the network analyzer. It should be noted that while the measured SE, in our experiment, is not identical to the plane wave, free space, SE, due to the confinement and wave polarization effects[100], it can be shown that the difference is negligible[85, 87].

2.3 Results and discussion

2.3.1 DC conductivity and percolation threshold

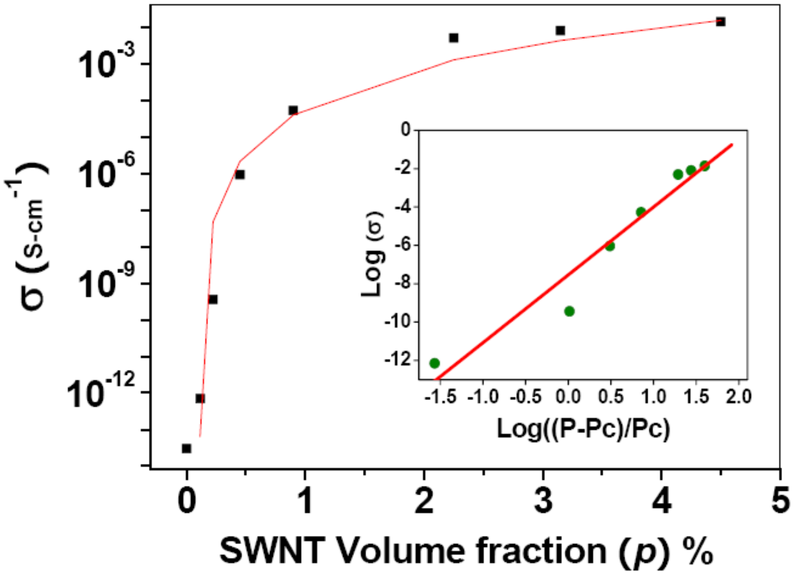

Figure 2-6 The electrical conductivity of the *functionalized* SWNT-RET composites follows a power law characteristic of percolation like behavior. The inset shows log-log plot of σ to $(P-P_c)/P_c$. (with a threshold volume fraction, $p_c \sim 0.11\%$ and an exponent of ~ 3.4).

We observed through DC electrical conductivity (σ) measurements on the SWNT-RET composite electrical percolation like behavior (Figure 2-6), which follows the laws of power, $\sigma \sim \sigma_0 (p - p_c)^t$, where p_c is the percolation threshold volume fraction (p) and t is a critical exponent. σ_o is a constant for a particular filler-polymer combination. The obtained values of p_c (~0.11%) and t (~ 3.4) from the best fit of the conductivity data to the log-log plots of the power laws in the inset to Figure 2-6, are appropriate for a thick film resistor configuration with elongated fibers[101]. It should be noted that at higher frequencies, capacitive coupling, in addition to continuous electrical paths between the nanotubes, can contribute significantly to the electrical conductivity [102].

2.3.2 Shielding effectiveness (SE) of SWNT/RET composites

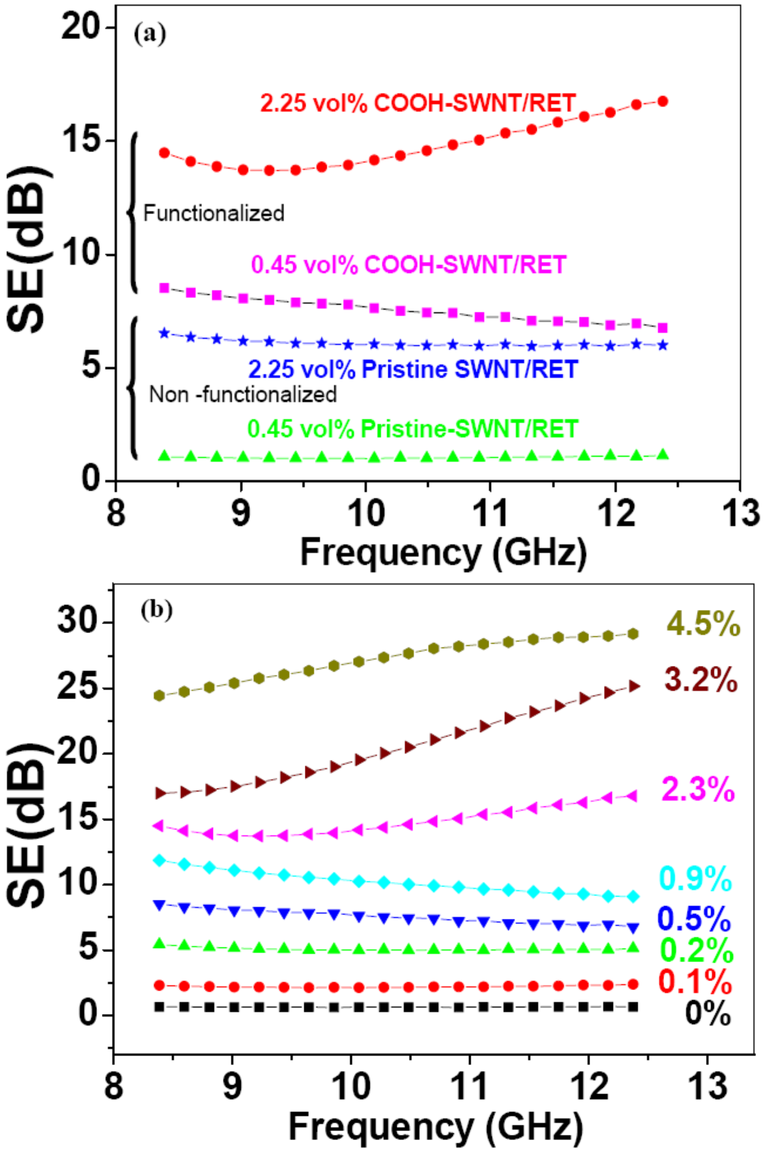

Figure 2-7 (a) An enhanced shielding effectiveness (SE) has been observed for the chemical functional group reaction enhanced SWNT-RET polymers (COOH-SWNT/RET) compared to non-functionalized SWNT-RET composites (Pristine SWNT/RET), and (b) increases with increased filling fraction of the SWNTs

We noticed that an order of magnitude higher shielding efficiency (SE) was obtained for the COOH- functionalized nanotubes compared to a dispersion of non-functionalized SWNTs in the RET polymer matrix (Figure 2-7 (a)). Such an effect is presumably due to the effect of uniform dispersion resulting in a better connectivity of the SWNT fillers. As expected, the SE increases with increasing amount of SWNT filler (Figure 2-7(b)).

2.3.3 Reflection and absorption of electromagnetic wave in CNT composites

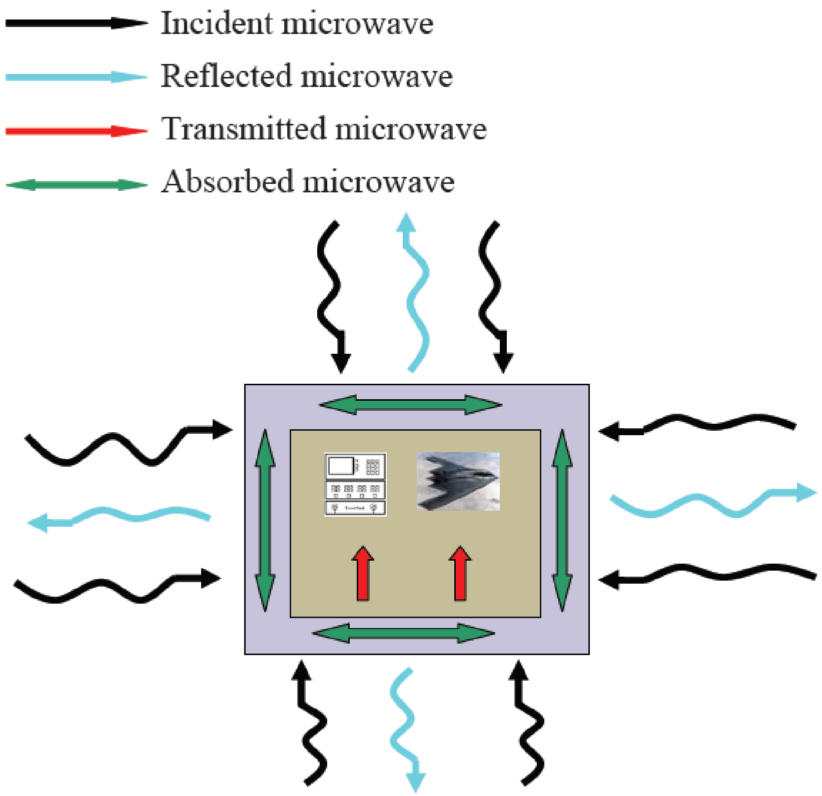

Figure 2-8 Schematic diagram for EMI shielding material: Black arrows indicate incident microwave (I). Blue arrows indicate reflected microwave (R). Red arrows indicate transmitted microwave (T). Green arrows indicated absorbed microwave (A).

Probing into the dependence of the SE *vs*. frequency, we notice (e.g., Figure 2-7), that at low (/high) CNT filling fractions the SE decreases (/increases) with frequency while exhibiting a minimum at intermediate filling fractions (e.g., ~ 2.3 volume % - Figure 2-7(b)).

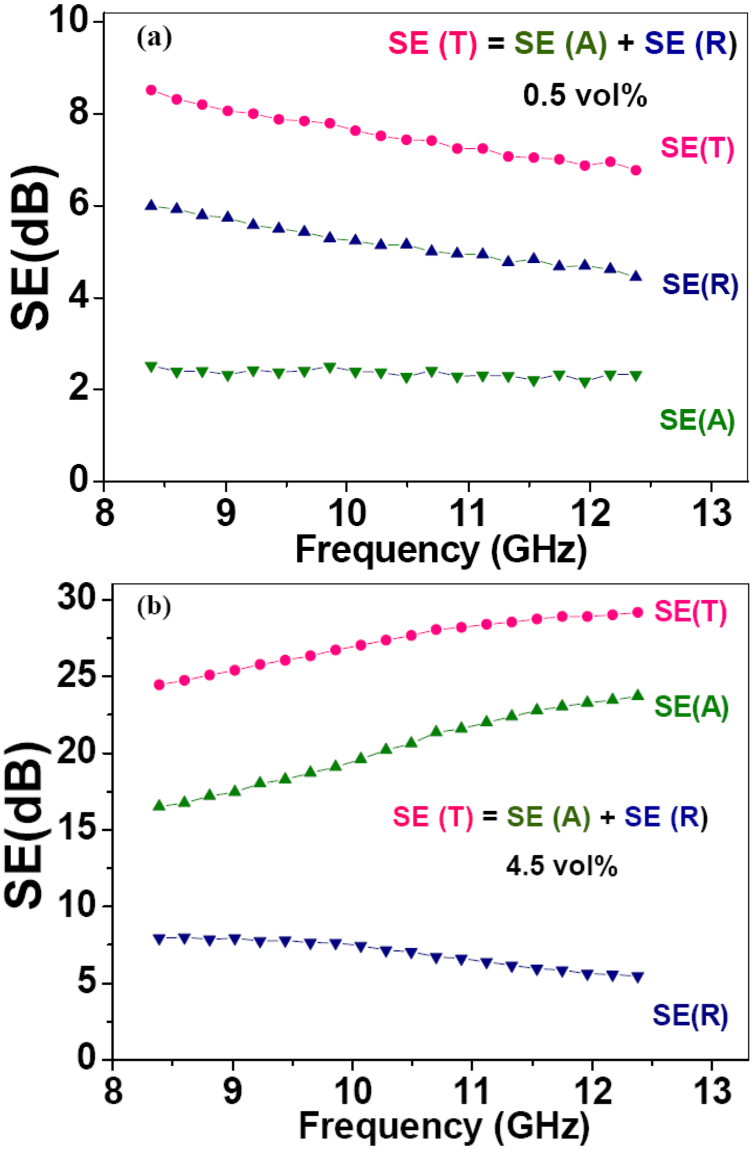

Figure 2-9 The total shielding efficiency, SE (Tot), can be decomposed into contributions from reflection, SE (R) and absorption, SE (A), through a consideration of the frequency (*f*) dependence. (a) Reflective losses dominate the total SE for low (~ 0.5 volume %) nanotube filling fractions, while (b) the absorption is more important at larger (~ 4.5 volume %) volume fractions.

One can understand such variations by considering the total effective shielding effectiveness, SE(Tot), of the composite as the sum of the contributions due to both the reflection (R) and the absorption (A) components, as SE (Tot)= SE (R) + SE(A), where SE(R) = -10 log(1-R) and SE(A) = -10 log[$\frac{T}{1-R}$][98, 103]. The R, A, and the T (transmission) were then obtained through the determination of the S-parameters using the vector network analyzer (schematic concept for R, T and T as shown Figure 2-8), where T = $|S_{21}|^2$, R = $|S_{11}|^2$, and A = 1 - $|S_{11}|^2$ - $|S_{21}|^2$. It was assumed here that the effect of multiple reflections on the SE is negligible for our considered composite thickness[81, 84]. It was then seen that the SE(R) > SE(A) for low volume % nanotube filling fractions – Figure 2-9 (a), while SE(A) > SE(R) for higher filling fractions – Figure 2-9 (b). It could be inferred that the cross-over from reflection dominated shielding to absorption dominated shielding occurs ~ 2.3 volume % (as seen in Figure 2-9 (b)). A preliminary explanation, and fit to experiment, where SE (R) *decreases* with frequency (*f*) while SE (A) *increases* with f was obtained through examining the form of R which varies as ~ $\log_{10}(\frac{\sigma}{f})$ through its dependence on the reflection loss and A, which is thickness (*t*) dependent, and varies as $t\sqrt{f\sigma}$ [104]. Simulations and experiments are in progress to explore such phenomena in more detail.

2.3.4 Aspect ratio affect of nanocomposites

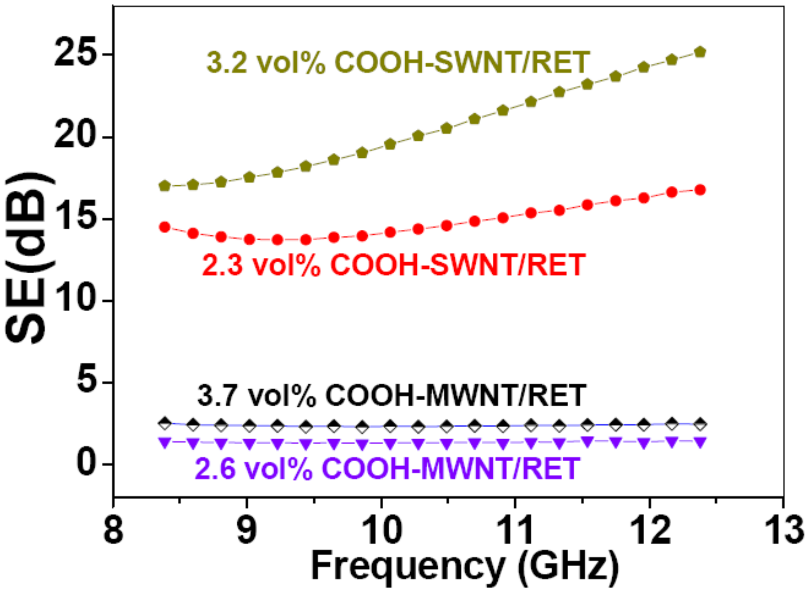

Figure 2-10 The shielding effectiveness is larger for the single-walled CNTs (SWNTs) compared to the multi-walled CNTs (MWNTs) and illustrates the predominant influence of the aspect ratio (SWNT ~ 880, MWNT ~ 30) in determining the percolation and the SE.

Interestingly, the SE is also much larger, almost by a factor of 100, for functionalized SWNTs compared to functionalized multi-walled nanotube (MWNT) – RET composites (Figure 2-10). We have noted previously that the aspect ratio of the MWNTs are smaller than the SWNTs, which implies (from Figure 2-1) reduced percolation and lower shielding effectiveness. We have experimentally observed that several variables such as (1) the aspect ratio of the CNTs, (2) electrical conductivity of SWNTs/MWNTs, and (3) the thickness of the composite, in addition to (4) frequency, can be used as knobs to determine the practical applicability of the CNT-RET polymer.

One example, as we have shown, is the way in which nanotube type and/or concentration modulates the reflective or absorptive components of EMI shielding.

2.4 Summary

Our study has provided an example of a nanotube (SWNT/MWNT)-polymer (e.g., RET) system which utilizes functional group interactions for achieving uniform dispersion with low electrical percolation concentrations and enhanced microwave shielding effectiveness. Analysis of the total observed EMI shielding was used for investigating the mechanisms of absorption and reflection in the composite, where a cross-over from reflection dominated shielding to absorption dominated shielding was observed at a CNT volume fraction of ~ 2.3%. It was also concluded that SWNTs were much more effective for shielding, compared to MWNTs. Preliminary experiments probing the mechanical characteristics of the proposed CNT-RET polymer composites have indicated increased tensile strength as a function of increasing volume fraction of the CNTs. In summary, our proposed scheme of using functionalized CNT-polymer composites together with our obtained results could be used as a basis for light-weight, high shielding efficiency materials for EMI applications.

The content for this chapter was taken from the published journal article: S. H. Park, P. Thielemann, P. Asbeck, P. R. Bandaru, “Enhanced electromagnetic interference shielding through the use of functionalized carbon nanotube-reactive polymer composites”, IEEE Transactions on Nanotechnology, TNANO-00013-2009.R1

Chapter 3. Dielectric properties of functionalized carbon nanotube composites

3.1 Introduction

Polymer composites containing conducting fillers[6] have been extensively investigated for various applications such as electromagnetic interference (EMI) shielding[16], electronic packaging[9], radar absorption[10], and high charge storage capacitors[11]. However, currently used composites require high filler to polymer loading ratios, which deteriorates the overall mechanical properties through deterioration of intrinsic matrix morphology. A possible way to ameliorate the above problems, through using low filler volume fractions, incorporates carbon nanotubes (CNTs)[84, 97, 102, 105] in composites. A concomitant large aspect ratio and tunable electrical conductivity would enable electrical percolation to be achieved at very small CNT volume fractions[102], with large shielding efficiencies being obtained, e.g., ~28 dB in CNT films[106] and ~16 dB in polyurethane/CNT composites[107] at 10 GHz. However, economic costs and clustering of the CNTs within the polymer matrix are issues that have to be overcome prior to large scale application.

In this paper, we tackle the clustering problem by considering the synthesis of well dispersed functionalized CNT composites. The superior nature of these composites, for EMI applications, is then characterized in the microwave frequency range of 8.2–12.4 GHz (*X*-band), used for civil and military communications with applications as diverse as weather monitoring, vehicular detection, air traffic control, and defense tracking[98].

3.2 Experimental procedures : Dielectric measurement set up

The electromagnetic properties of the CNT-RET nanocomposites, as measured through the *S*-parameters[98] (S_{ij}), were recorded in the microwave frequency range (8.2-12.4 GHz: X-band) using a vector network analyzer (Agilent 5242A PNA-X) as shown in figure 3-1. The composite loaded sample holder was inserted between two 15 cm lengths of WR-90 X-band waveguide to mitigate the near-field effects of the coax to waveguide transitions. The determination of S_{11} and S_{21} enables the calculation of the complex permittivity ($\varepsilon = \varepsilon' + j\,\varepsilon''$) and permeability ($\mu = \mu' + j\mu''$), where $j = \sqrt{-1}$, through[108]:

$$S_{11} = \frac{(1-\Gamma^2)z}{1-\Gamma^2 z^2} \qquad (1)$$

$$S_{21} = \frac{(1-z^2)\Gamma}{1-\Gamma^2 z^2} \qquad (2)$$

Equations (1) and (2) permit the determination of the reflection coefficient,

$\Gamma = \frac{\sqrt{\frac{\mu_r}{\varepsilon_r}-1}}{\sqrt{\frac{\mu_r}{\varepsilon_r}+1}}$ and the transmission coefficient z, (= $e^{-j\frac{\omega}{c}\sqrt{\mu_r\varepsilon_r}}$), from which ε_r and μ_r were ascertained[109], with an error of at most 7%.

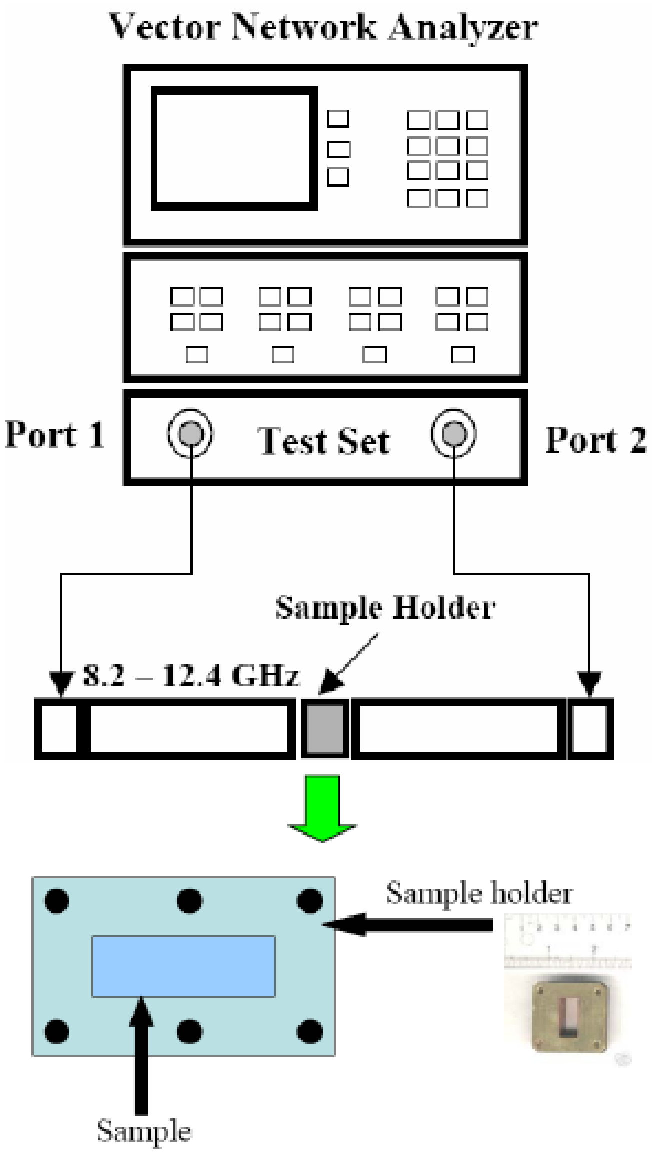

Figure 3-1 Schematic diagram of setup for *S*-parameters measurements[21].

3.3 Results and discussion

Base on chapter 2, we indeed observed a more uniform dispersion using functionalized SWNTs for both low (Figure 3-2(a)) and high (Figure 3-2(b)) CNT filling fractions, through Scanning Electron Microscopy (SEM: Phillips XL30) images of the fracture surfaces of the composites, in comparison to the clumping observed (Figure 3-2(c)) when un-functionalized nanotubes were mixed into the polymer. Uniform dispersion was also seen for functionalized MWNTs. (Figure 3-2(d))

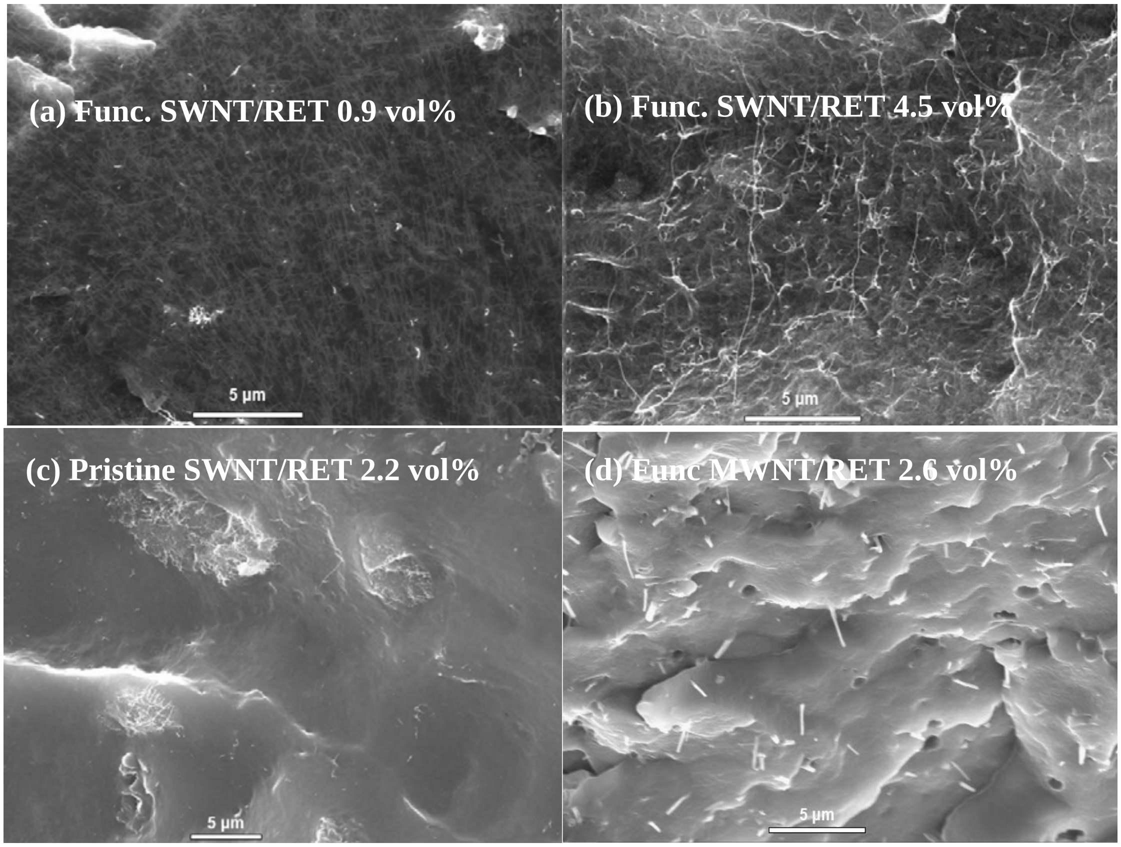

Figure 3-2 SEM micrographs of **(a)** 0.9 volume % and **(b)** 4.5 volume % *functionalized* SWNT-RET composites, **(c)** 2.2 volume % of *non-functionalized* SWNT-RET composites.

3.3.1 Real and imaginary permittivity

The frequency variation of the real (ε′) and imaginary (ε″) permittivity of the functionalized SWNT-RET composites, as a function of SWNT concentration (ϕ_{CNT}) is depicted in Figure 3-3 (a) and (b), respectively. It can be seen that composites constituted of functionalized SWNTs have ε' (/ε'')~ 5 (/25) times greater than composites composed of (i) pristine SWNTs, presumably due to the better filler dispersion, and ε'(/ε'') ~ 10 (/300) times larger than (ii) functionalized MWNT-RET composites, attributed to a larger aspect ratio.

While an increase in ε' with increased SWNT volume fraction could be due to the formation of an increased number of SWNT-RET dielectric-SWNT capacitors, the increase in ε'' (= Re [$\frac{\sigma}{\omega\varepsilon_o}$]) was mainly due to an increased electrical conductivity (σ), at increased SWNT filling fractions. Additionally, enhancement of ε'', through dielectric loss, could be also related to interfacial polarization at the grain boundary and subsequent dipole reorientation facilitated by the formation of an inter-phase region at the CNT-RET interface[110]. Preliminary modeling of the dielectric constant of the nanotube composites (ε_c) was done through the law of mixtures[110], i.e.,

$$\varepsilon_c = \phi_{CNT}\varepsilon_{CNT} + (1 - \phi_{CNT})\varepsilon_{RET} \qquad (3)$$

where ε_{CNT} (/ε_{RET}) and ϕ_{CNT} (/1-ϕ_{CNT}) are the complex dielectric constants and volume fractions) of the CNT fillers (/RET polymer matrix), respectively. A good agreement (± 10%) with the experimental values was obtained for ε_c.

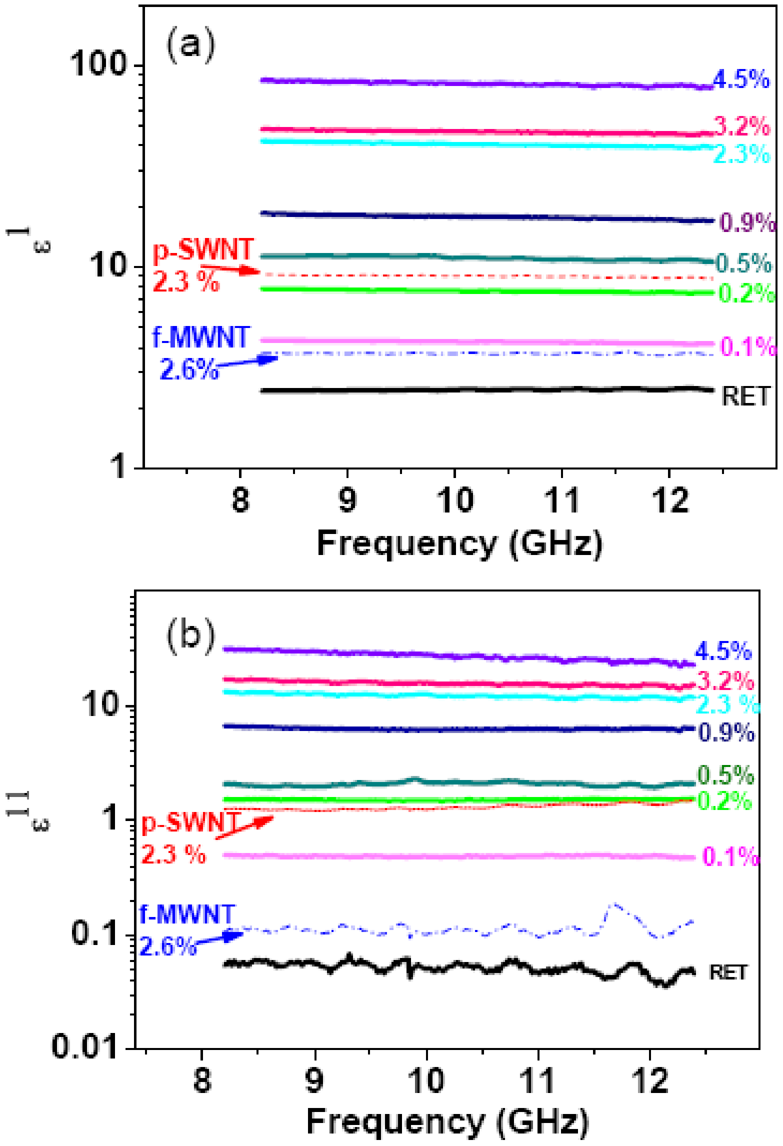

Figure 3-3 The (a) real - ε', and (b) imaginary - ε'' components of the dielectric constants of functionalized SWNT-RET composites (numbers in % indicate volume fraction of SWNTs), are larger than pristine SWNT (p-SWNT) and functionalized MWNT (f-MWNT)-RET composites.

3.3.2 DC conductivity, AC conductivity and SE

The four-wire resistance method was then used to measure the electrical conductivity (σ) of the CNT-RET composites. The DC conductivity (σ_{dc}) of the composites measured as a function of the incorporated volume fraction of functionalized SWNTs is shown in Figure 3-4(a) and fit to a percolation theory[111] based expression of form

$$\sigma \sim \sigma_0(\phi_{CNT} - \phi_c)^t \qquad (4)$$

where ϕ_{CNT} is the SWNT volume fraction, ϕ_c the percolation threshold volume fraction and t a critical exponent. σ_o is a constant. From the fit, the values of ϕ_c (~0.11%) and t (~ 3.4) were obtained. While t seems to be appropriate to a thick film resistor configuration with elongated fibers[101], the observed ϕ_c is one of the *lowest* reported in literature. We calculated from excluded volume based percolation theory[82], that for the given SWNT aspect ratio (~ 880), a theoretical ϕ_c of 0.1 vol% which is in excellent agreement with our results. The low ϕ_c also implies a correlated bond model of percolation[111], with SWNT interactions. Supporting evidence for such interactions was obtained through the determination of the AC conductivity (σ_{AC}) of the composites (calculated[102] through $\sigma_{AC} = 2\pi f\varepsilon_0\varepsilon''$, at a given frequency f with $\varepsilon_0 = 8.854 \cdot 10^{-12}$ C^2/Nm^2) and is shown in Figure 3-4(b). The following was noted: (1) σ_{AC} varies *linearly* with ϕ_{CNT}, (2) $\sigma_{AC} > \sigma_{DC}$, even below ϕ_c and, that (3) σ_{DC} approaches σ_{AC} at high (> 4 vol %) filling fraction of the SWNTs.

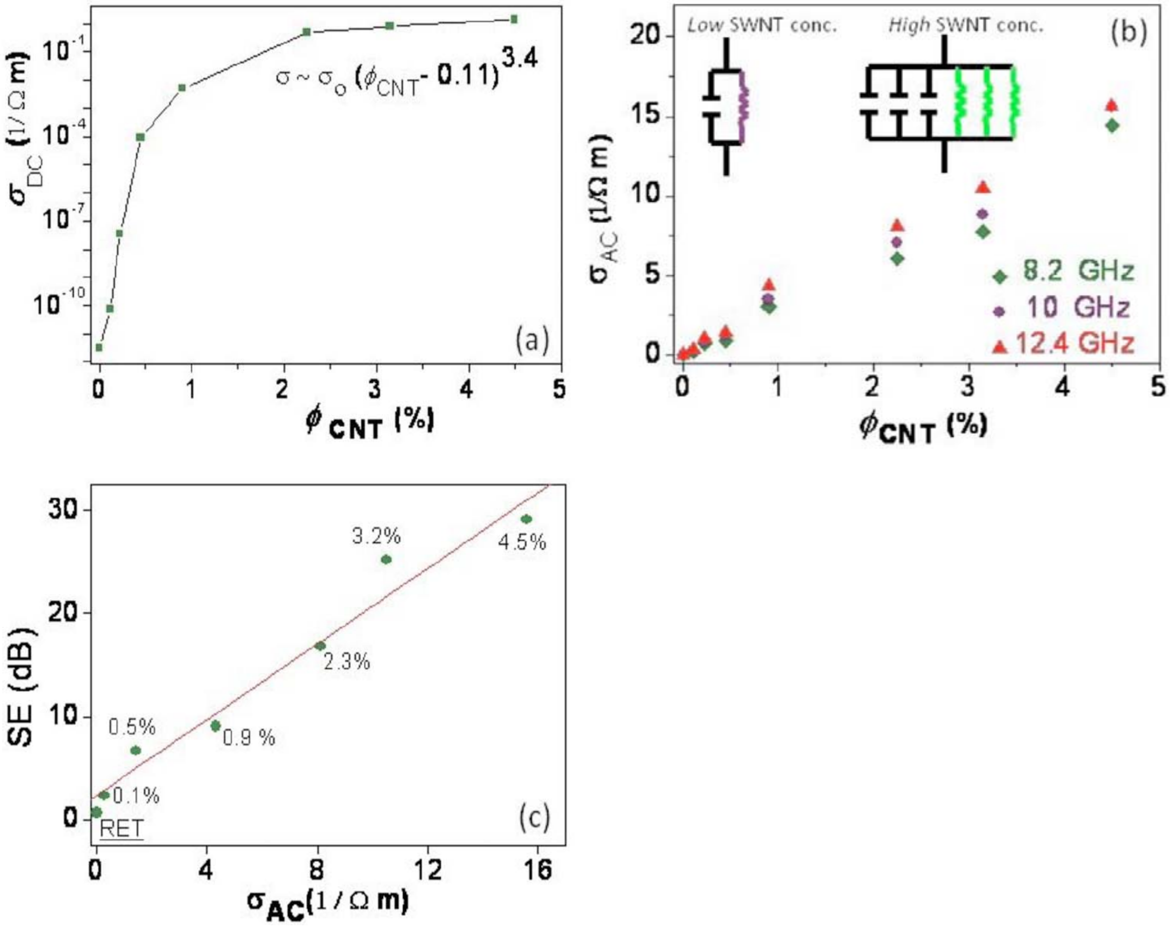

Figure 3-4 (a) The DC conductivity, σ_{DC}, of functionalized SWNT-RET composites follows a power law characteristic of percolation like behavior (with a threshold volume fraction, $\phi_c \sim 0.11\%$ and an exponent of ~ 3.4). (b) The AC conductivity, σ_{AC}, of the SWNT-RET composite increases linearly with SWNT volume fraction (ϕ_{CNT}), and frequency, at a particular ϕ_{CNT}. The inset shows the parallel resistor-capacitor combination used to model σ_{AC}. (c) The σ_{AC} can be used as a predictor of the shielding effectiveness (SE) of the nanocomposites (numbers indicate ϕ_{CNT}) - data obtained at 12.4 GHz. The polymer matrix reference is indicated by RET.

These observations indicate a frequency dependent mechanism of electrical conduction, which was sought to be understood through a very simple model of parallel resistors and capacitors formed in the nanocomposite[102] –Figure 3-4(b)inset. In this model, the SWNTs contribute to the electrical resistance while the polymer matrix serves as the capacitor dielectric and contributes to the AC conductance.

As the SWNT concentration in the matrix increases, equivalent to an increasing number of parallel resistors and capacitors, the net resistance and capacitive impedance ($X_c = \left|\frac{1}{2\pi f C}\right|$) decreases due to the availability of several alternative electrical conduction paths. Consequently, both σ_{DC} and σ_{AC} increase, with a diminishing difference at higher f. Such a parallel conduction model was also supported from the linear relationship of the shielding effectiveness (SE), which was independently obtained from the S-parameter measurements[98] to σ_{AC} (Figure 3-4(c)), through SE = -10 log (T), where T ($\equiv |S_{21}|^2$) is the transmittance. We also observed higher values of SE at a lower loading fraction of SWNTs (i.e., ~ 30 dB at 4.5 volume % of SWNTs) compared with literature, e.g., < 15 dB with 15 % SWNTs at 1 GHz[84], with 11.6 % SWNTs at 8 GHz[86], and ~ 20 dB with 8.6 % SWNTs at 8 GHz[87], presumably due to the uniformity of dispersion. Additionally, our values are comparable to those obtained in carbon nanotube films, of ~ 28 dB at 10 GHz[88].

3.4 Summary

In summary, we have seen that functionalized SWNTs, with a high aspect ratio, favor uniform dispersion into an RET polymer matrix and have a major influence on the electromagnetic properties. The relationship of ε'' to σ_{AC} was used as a metric for the EMI shielding effectiveness and understood in terms of a parallel resistor-capacitor model. Future work would focus on the validity of the model and the utility of uniformly dispersed composites for various applications.

The content for this chapter was taken from the published journal article: S. H. Park, P. Thielemann, P. Asbeck, P. R. Bandaru, “Enhanced dielectric constants and shielding effectiveness of uniformly dispersed functionalized carbon nanotube composites”, Applied Physics Letters, 94, 243111 ,2009

Chapter 4. Enhanced mechanical properties of functionalized carbon nanotube composites

4.1 Introduction

Polymer composites containing conducting fillers[6] such as carbon black[112], carbon fiber, and metal fiber have been extensively investigated for multi-functional applications including structural reinforcement[7], electromagnetic interference shielding[8], electronic packaging[9], radar absorbing material[10], and as high charge storage capacitors[11]. A concomitant enhancement in the mechanical properties can also be observed in the composites, e.g., through load transfer from low elastic modulus (*E*) polymer matrix to a high *E* filler[113]. However, there is a limit to the impregnation of polymers with filler material, beyond which there could be embrittlement. Generally, high aspect ratio fillers would favor electrical percolation at lower volume fractions and are desirable. Carbon nanotubes (CNTs) offer a most attractive option in this regard, primarily due to their extremely large aspect ratio - as high as 10^6 [78]- along with a large interfacial area, > 1300 m^2/g [114], and also facilitate load transfer over a longer length along with superior shear strength, Additionally, the CNT surfaces and interfaces can be made to interact suitably with the polymer matrix through the use of suitable coupling agents[115].

However, there are still several challenges to the utilization of CNTs, e.g., (a) aggregation and bundling leading to a non-uniform dispersion, along with (b) poor interfacial bonding of the nanotubes with the polymer matrix, both of which lead to variable performance of the composites, along with the (c) high cost of CNTs. Consequently, while single walled CNT (SWNT) and multi-walled CNT (MWNT) composites have been reported [116-119] to yield enhanced elastic moduli and tensile strengths, the values of these parameters greatly diminishes beyond a certain loading, e.g., ~ 0.6 % in phenol-SWNT composites[120], or polypropylene-SWNT composites[119]. It is also frequently seen that while CNT loading nanotubes leads to an increased elastic modulus (*E*)/ tensile strength (*UTS*) for the composite, the toughness and strain to failure often decrease [121, 122].

Consequently, we suggest a possible method to enhance the mechanical properties of nanotube reinforced polymer composites through the influence of homogeneous dispersion and enhanced nanotube-polymer interface bonding, accomplished through mutual localized chemical reactions[76, 123] between a functional group on the SWNTs with functional groups on the polymer. We then show that *UTS* and *E* of such functionalized SWNT-polymer nanocomposites are superior to those of unfunctionalized SWNT-polymer composites, at identical CNT filling fractions. Additionally, we show that simultaneous toughening and strengthening could be achieved when the average length of the uniformly dispersed SWNTs is adequate to bridge incipient cracks. We then propose models to explain the observed mechanical behavior, considering the effects of CNT agglomeration, aspect ratio, and the effect of intra-CNT filler interactions in reducing the toughness beyond a certain critical CNT concentration in the matrix.

4.2 Experimental Procedure

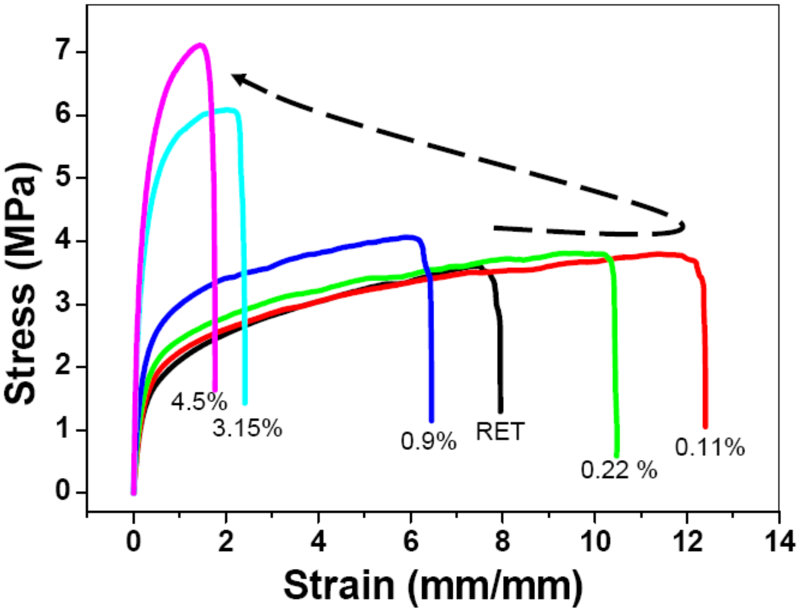

Figure 4-1 Stress-strain curves of functionalized SWNT-RET composites with different loading of nanotubes. Composites with low nanotube loading (below 0.9 vol%) show ductile behavior with high elongation whereas after 0.9 vol% loading composites show stiff behavior with high strength.

The mechanical properties of CNT-RET composites, in the form of 25 mm X 9 mm X 0.7 mm test samples, were measured at room temperature using a electro-mechanical testing machine (INSTRON 3342), incorporating a tension/compression transducer(load cell) operated at a crosshead speed of 30 mm/min. At least five specimens were tested to obtain average values. Scanning electron microscopy (SEM) (Phillips XL30 ESEM) was used to probe the morphology of the CNT-RET composites, prior to and subsequent to mechanical measurement, where samples were quenched in liquid nitrogen and broken to achieve a fracture surface. Typically, the surfaces were coated with a thin Au/Pd over layer (5 – 10 nm) to increase imaging contrast.

4.3 Results and discussion

4.3.1 Tensile strength and elastic modulus of nanocomposites

The examination of the stress-strain curves of the nanocomposites with varying loading of SWNTs, as depicted in Figure 4-1, seems to indicate transitions in the mechanical behavior at filling fraction of ~ 0.9% and 0.11 vol%, through an increase in the *E* and reduction in the toughness, respectively. The variation of the *UTS*, which was noted through the peak of the stress-strain curves, as a function of the SWNT volume fraction is shown next in Figure 4-2 for both –COOH functionalized and unfunctionalized SWNT-polymer composites. The beneficial effects of functionalizing the SWNTs through a uniform and linear increase of the *UTS* is evident, e.g., at 4.5% the *UTS* is more than doubled over the untreated RET polymer and is also substantially higher than for the case of unfunctionalized SWNT dispersion. While the reason for the *UTS* maxima in the latter case is presently not understood; inhomogeneous SWNT dispersion- Figure 2-4(c) – is possibly important. From comparison with literature, it was seen that the *UTS* enhancement is much higher than could be accomplished at an equivalent volume fraction through the use of platelet clay/talc fillers of a smaller aspect ratio (~5) and which are weakly bonded to the RET [124]

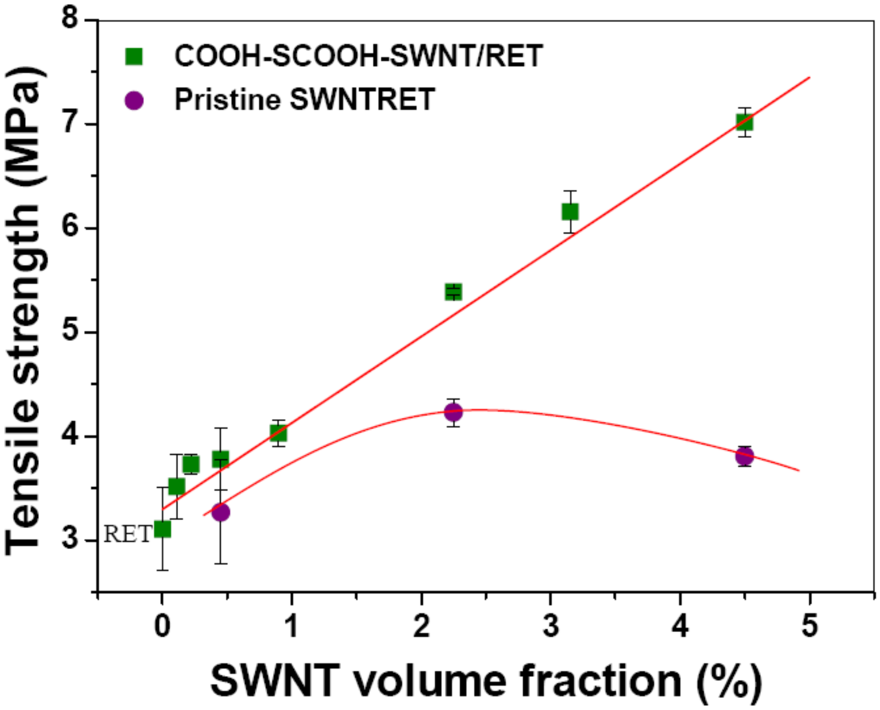

Figure 4-2 Tensile strength of the functionalized SWNT-RET composites (■) and pristine SWNT-RET composites (●) with different loading of SWNTs

The variation of the *E* with SWNT volume fraction - figure 4-3- again compares the effect of functionalization and contrast with the use of MWNTs. While functionalization implies a net strengthening of the polymer matrix, the larger aspect ratio of the SWNTs (~ 880) compared to MWNTs (~ 30) possibly leads to a greater amount of stress transfer for a given strain.

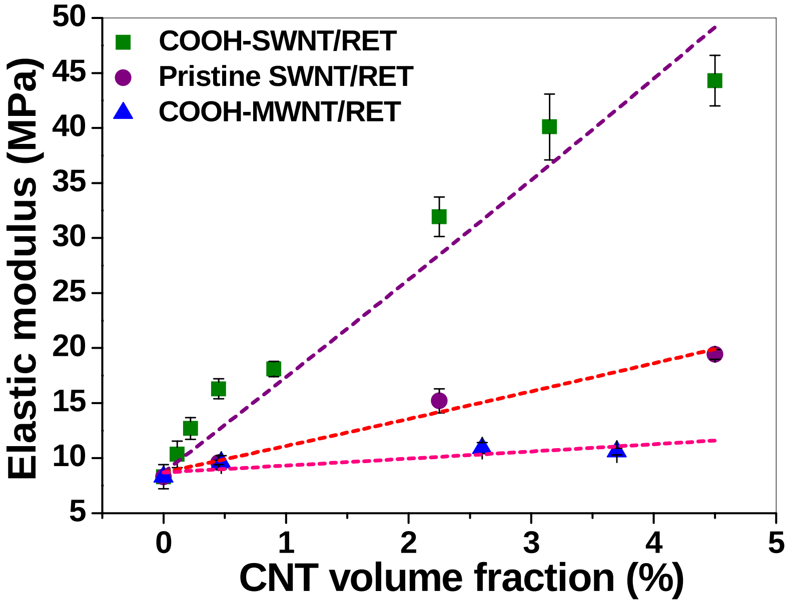

Figure 4-3 Elastic modulus of functionalized SWNTs (■) and MWNT (▲) – RET composites and pristine SWNT-RET (●) composites with different loading of nanotubes. Each experimental data were fitted by the the modified Halpin-Tsai equation.

To predict the *E* of the nanocomposite, we consider its mechanical properties to be akin to those of a semi-crystalline polymer with the nanotubes as a constituent reinforcement phase. Such a system is often modeled through the Halpin-Tsai system of equations [125], where it is assumed that the *E* is insensitive to the matrix and the nanotube Poisson ratios. In this case, the CNTs, with intrinsic elastic modulus, E_{NT} (~ 700 GPa for 5 nm bundle of SWNTs [126]) and at a volume fraction-v_f, are modeled to serve for enhancing the effective elastic modulus of the polymer matrix (E_m) through:

$$E = \frac{1 + c\eta v_f}{1 - \eta v_f} E_m \quad \text{where} \quad \eta = \frac{\left(\frac{E_{NT}}{E_m}\right) - 1}{\left(\frac{E_{NT}}{E_m}\right) + c} \tag{1}$$

The parameter c was introduced a measure of reinforcement (CNT) geometry and modeled through, $c = 2\left[\frac{L_{NT}}{r_{NT}}\right] \times p$, where L_{NT} and r_{NT} are the CNT length and radius, and p is related to the degree of CNT aggregation. We have introduced p as a semi-empirical parameter, related to the extent of aggregation, as depicted in Figure 4-4**.** Note that p as defined is a rough measure of the reduction of load transfer and could also account for curvature [116, 120, 121] that is often observed in nanocomposite processing, e.g., Figure 3-2 (b)

A best fit of the E to v_F - figure 4-3- indicated p = 18 for functionalized SWNT nanocomposites whereas p = 67 for unfunctionalized SWNT impregnated polymer composites. Consequently, a *four-fold* increase in the degree of aggregation is indicated in the latter, *cf,* figures 2-4 (b) and figure 2-4(c). For functionalized MWNT, p is ~ 10 indicating less aggregation. However, due to small aspect ratio (~30), c parameter is much smaller than SWNT.

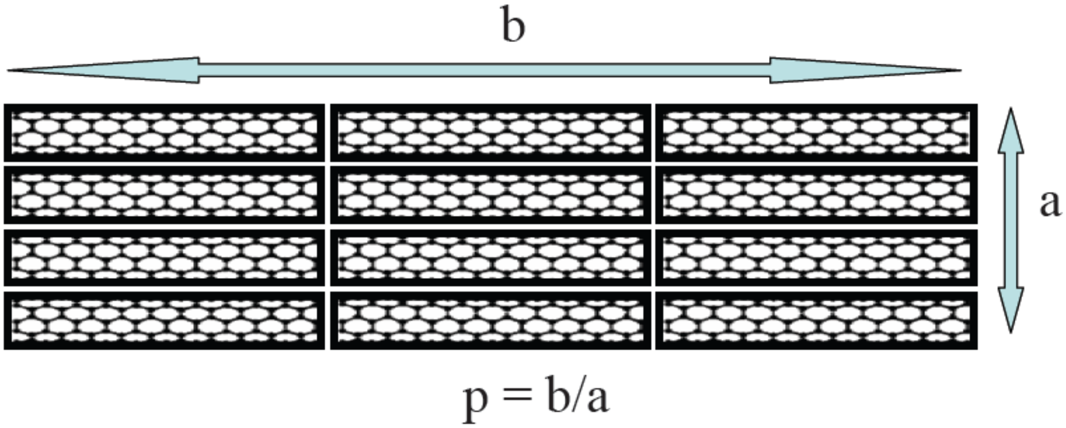

Figure 4-4 Schematic diagram for constants p related to the degree of nanotubes aggregation. Depending on nanotubes status such as degree of exfoliation, dispersion and curved shape, p (= b/a) values can be different. A larger p could be indicative of CNT aggregation in the polymer.

4.3.2 Toughness and elongation of nanocomposites

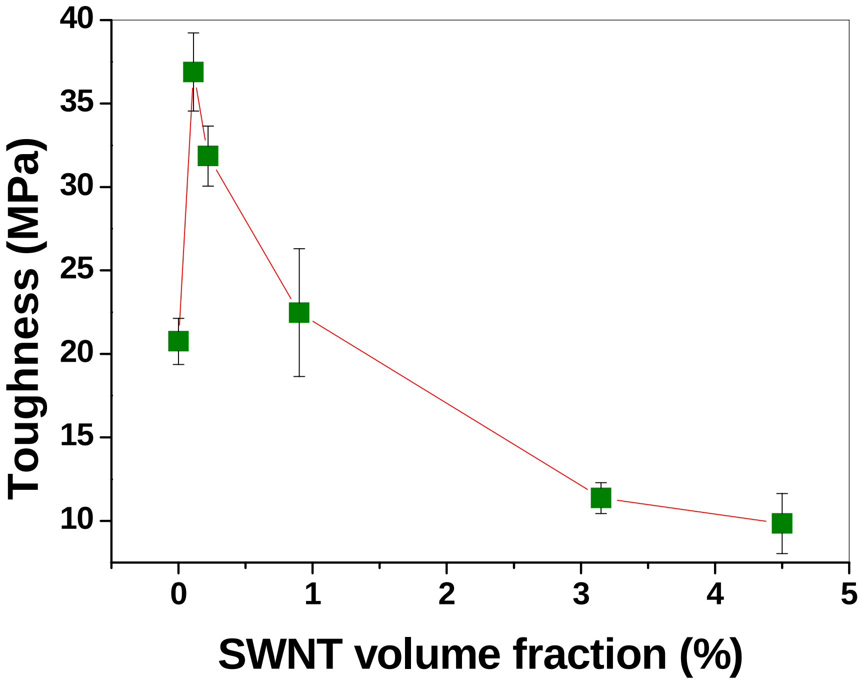

Figure 4-5 Toughness of functionalized SWNT-RET composites with different loading of nanotubes

As remarked earlier, and as seen through the stress-strain curves in figure 4-1 a maximum in the toughness (defined as the area under the stress-strain curves) occurs at ~ 0.11 % for the functionalized SWNT-RET composites - Figure 4-5. A physical mechanism for the initial increase is probably due to the observed incipient crack (< 4.3 μm, corresponding to the observed CNT bundle length) bridging by the CNTs [127] [120, 128]– Figure 4-6, preventing polymer failure [129]. The observed morphology could be due to the location of the functional groups on the CNTs, mostly situated at the ends[130]. Enhanced stress ultimately results in the separation of the SWNTs from the matrix [131]. A subsequent decrease in the toughness, beyond 0.11 %, could then arise due to the CNTs forming a percolating network and dominating the properties of the nanocomposite. Indeed, we have seen in separate experiments probing the electrical conductivity of the studied nanocomposites that percolation is achieved at 0.11 volume% and it is tempting to suggest a close correspondence to the value of the toughness maximum. Further studies to probe the percolation thresholds for electrical and mechanical properties are in progress to confirm the above hypothesis.

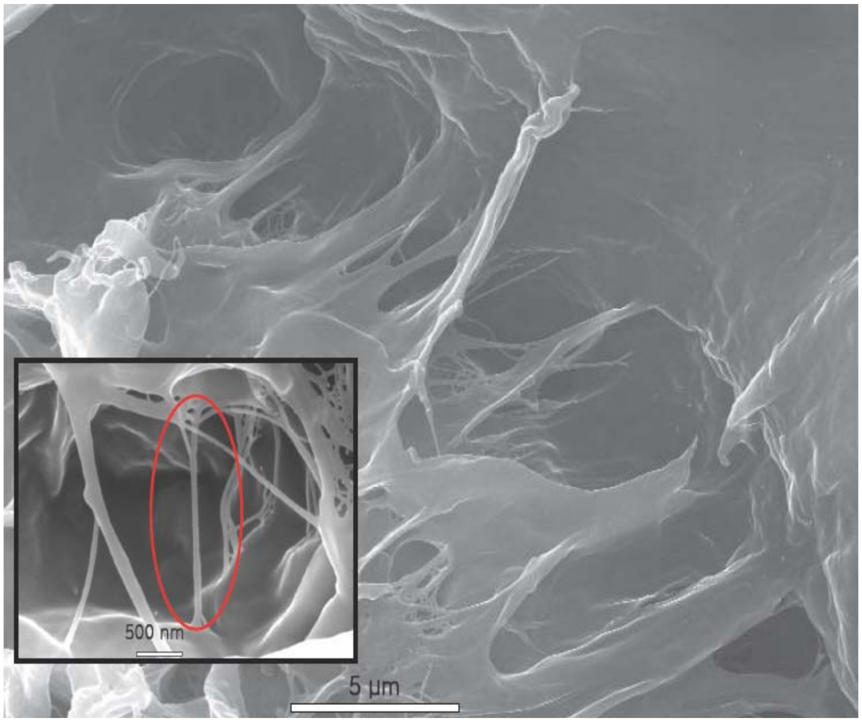

Figure 4-6 SEM images of functionalized SWNT-RET composites after tensile testing. Nanotube bundles work as bridge (red circle) and were pulled out tightly from the crack of the matrix that is different with figure 1(b) (: freeze fracture image without tension)

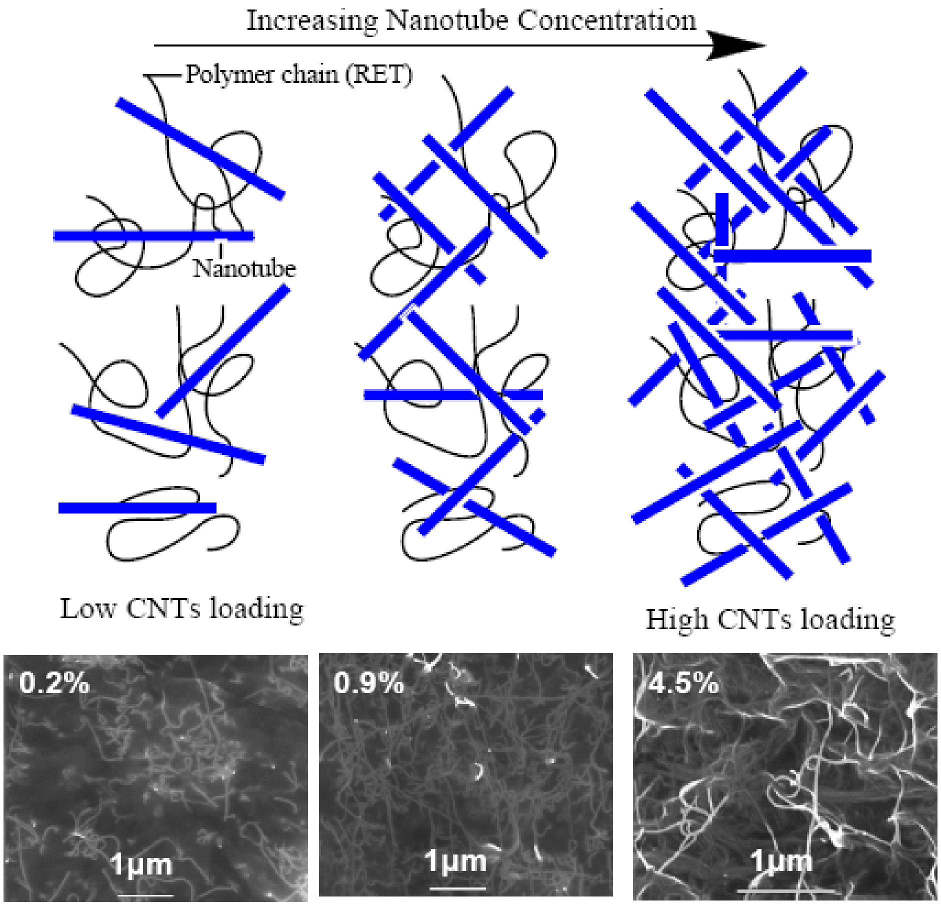

Figure 4-7 Schematic diagram of nanotube composites depend on nanotube concentration. At low CNTs loading (left top and bottom), toughness and elongation are increased. Whereas, at high CNTs loading (right top and bottom), toughness and elongation are decreased due to excess of covalent bonding between CNTs and polymer chain .

Consequently, with E_{CNT} (~ 700 GPa) >> E_m (~ 8.31 MPa), the toughness is reduced. A simple model of such a transition in the toughness behavior of the toughness is shown in Figure 4-7. At high CNT loading, while the *E* and *UTS* are enhanced the flexibility of the polymer is shown to be reduced. It would be interesting to consider whether the toughness maxima could be tailored, i.e., increase/decrease, through an decrease/increase in the aspect ratio, and through modifying the CNT-polymer interface[67].

We summarize the salient physical properties of functionalized SWNT-RET polymer composites in Table 4-2. It is seen that at low SWNT volume fractions, the enhanced toughness could be used for fabricating energy dissipation/damping material while higher volume fractions, with superior *E* and UTS along with enhanced electrical conductivity[132] can be used for applications that require strength, e.g., electromagnetic interference (EMI) shielding materials[133].

Table 4-2 Mechanical and electrical properties of functionalized SWCNT/RET composites

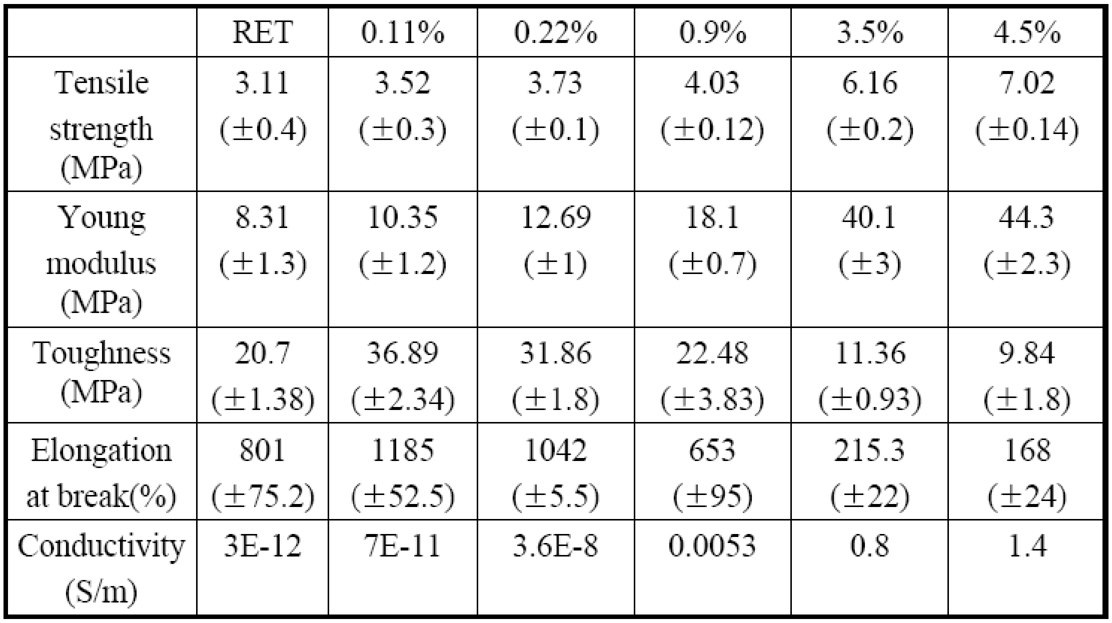

	RET	0.11%	0.22%	0.9%	3.5%	4.5%
Tensile strength (MPa)	3.11 (±0.4)	3.52 (±0.3)	3.73 (±0.1)	4.03 (±0.12)	6.16 (±0.2)	7.02 (±0.14)
Young modulus (MPa)	8.31 (±1.3)	10.35 (±1.2)	12.69 (±1)	18.1 (±0.7)	40.1 (±3)	44.3 (±2.3)
Toughness (MPa)	20.7 (±1.38)	36.89 (±2.34)	31.86 (±1.8)	22.48 (±3.83)	11.36 (±0.93)	9.84 (±1.8)
Elongation at break(%)	801 (±75.2)	1185 (±52.5)	1042 (±5.5)	653 (±95)	215.3 (±22)	168 (±24)
Conductivity (S/m)	3E-12	7E-11	3.6E-8	0.0053	0.8	1.4

4.4 Summary

We have proposed that the use of localized chemical reactions, enabling the interaction of the functional groups on the SWNTs with the polymer matrix, helps in the homogenous dispersion of the nanotube reinforcements. Our method can be used for any polymer with epoxide ring structure, such as diglycidyl ethers[76, 134]. Consequently, the interfacial bonding and load transfer is enhanced and enables enhancement in the *E* and *UTS* compared to when unfunctionalized SWNTs are used for filler material. We have also seen that a larger aspect ratio is imperative in enhancing the strength, through comparison with functionalized MWNT reinforced composites. A toughness maximum is indicated at low nanotube volume fractions, mainly caused through incipient crack bridging by the CNTs. However, the toughness is diminished at increased CNT loading due to mechanical percolation effects. Future work would focus on further understanding such effects *vis-a-vis* SWNT volume fraction. It should also be possible to introduce defects at various locations, other than the ends to further improve the toughness [135].

The content for this chapter was submitted to Carbon: S. H. Park, P. R. Bandaru, “Enhanced mechanical properties of polymer functional group hybridized carbon nanotube composites” (2009)

Chapter 5. Enhanced dielectric constants and electromagnetic shielding in polymer nanocomposites through the use of coiled carbon nanotubes

5.1 Introduction

A change in structure and morphology, at the nanoscale, could have a profound influence on macroscopic characteristics, through the paradigm of "function follows shape". For example, in the case of carbon based nanostructures, nonlinear helical and coiled carbon nanotubes (CCNs)/nanowires (CCNWs)[136] have been proposed for a variety of applications such as electrical inductors[137], spring-like mechanical elements for cushioning and energy dissipation[138, 139] etc. In this study, we suggest yet another application, based on experimental evidence, that the incorporation of coiled structures could enhance the intrinsic electromagnetic properties, e.g., the dielectric constants and the electromagnetic interference (EMI) shielding, of polymer matrices.

5.2 Experimental procedures

We have previously shown that In and Sn based catalysts could be used to promote helical CCNs/CCNWs growth in chemical vapor deposition (CVD) based processes[136] (Figure 5-1(a)). The constituent tube diameters were quite uniform in the 20~25 nm range, with a pitch of ca.1 μm. A tentative model, incorporating thermodynamic and kinetic factors, underlying their growth mechanism has also been proposed[140]. In the present study, we have incorporated such helical CCNs and mixed carbon nanotubes (MCNs : linear + coiled nanotube) (Figure 5-1(b)) into polymer matrices at various volume fractions. In MCNs, from various SEM images, 50% are coiled shape and 50% are linear shape. For comparison, we also introduce linear CNTs, i.e., both single walled (SWNTs: average diameter 1-2 nm, length 5-20 μm) and multi-walled nanotubes (MWNTs: (average diameter 140 nm, length 5-10 μm). Base on our previous concepts, we successfully fabricated CCN composites (2 wt%) with the uniform dispersion condition as shown Figure 5-1 (c) and (d).

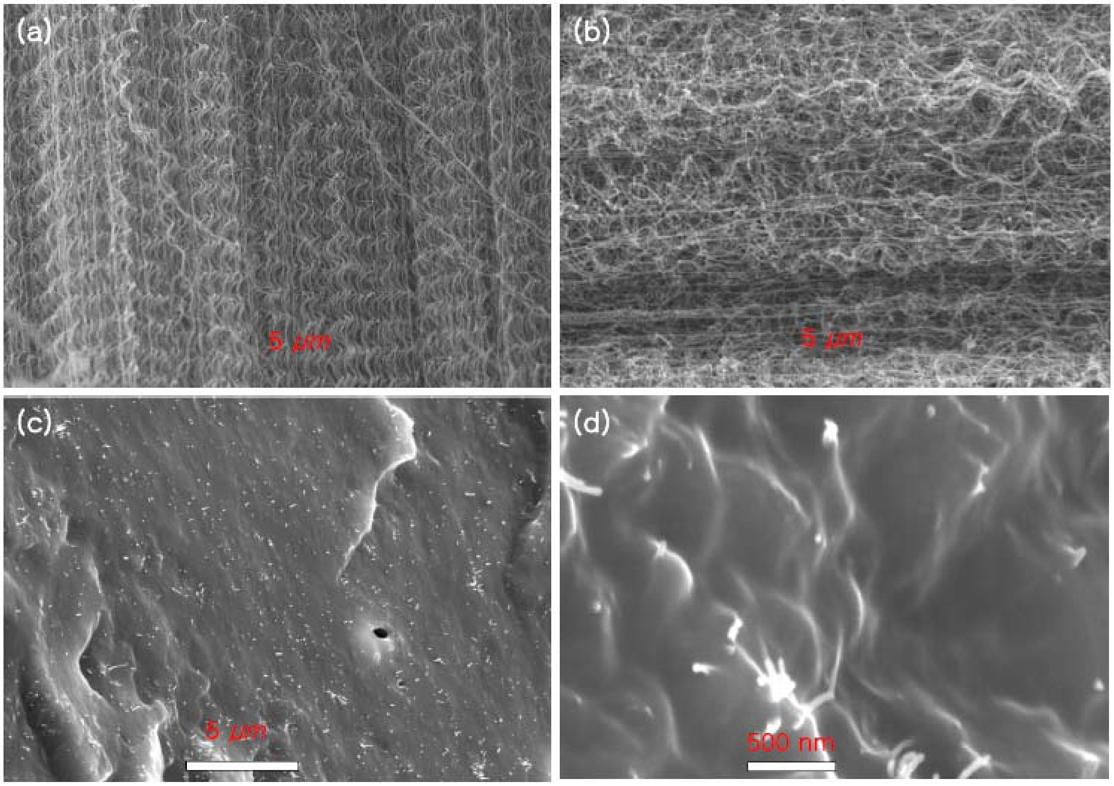

Figure 5-1 Scanning Electron Microscope (SEM) images (a) Highly aligned coiled carbon nanotubes (CCNs) with nearly identical diameter and pitch. (b) mixed carbon nanotubes (MCNs : coil + linear carbon nanotubes) (c) 2 wt% of CCN-RET composite having uniform dispersion condition. (d) High resolution image of CCN-RET composite

5.3 Results and discussion

For a detailed understanding of the electromagnetic response of the CCN/MCN composites, first we ensured that the dc electrical conductivity (σ_{DC}) was similar ~ 10^{-3} $\Omega^{-1}m^{-1}$ for SWNT, MCN and CCN case shown in Figure 5-2.

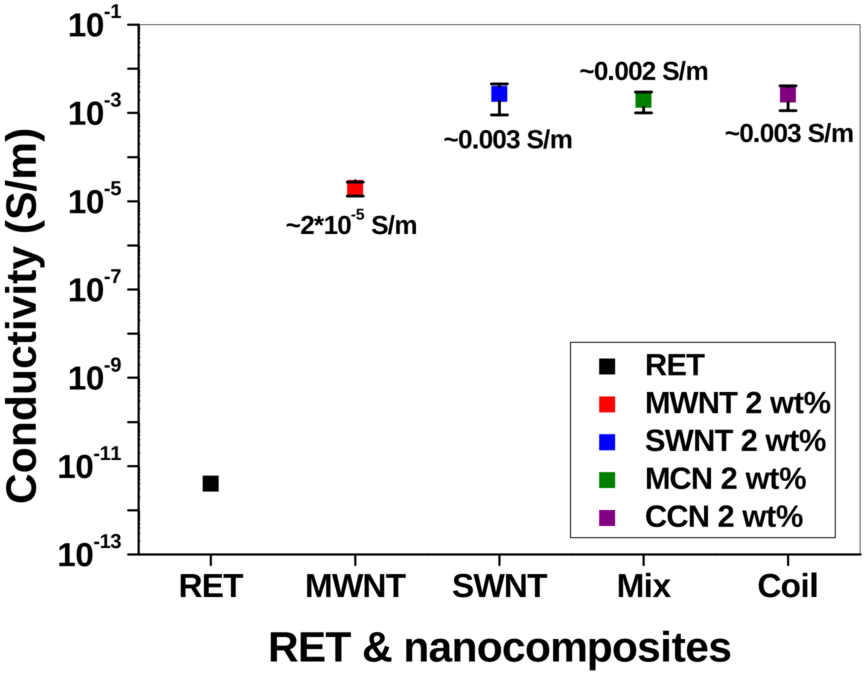

Figure 5-2 The DC conductivity of nanotube composites with same 2 wt% filling. (Filler: MWNT, SWNT, MCN, CCN)

With same procedures shown Chapter 3, real and imaginary permittivity of nanotube composites are shown in Figure 5-3.

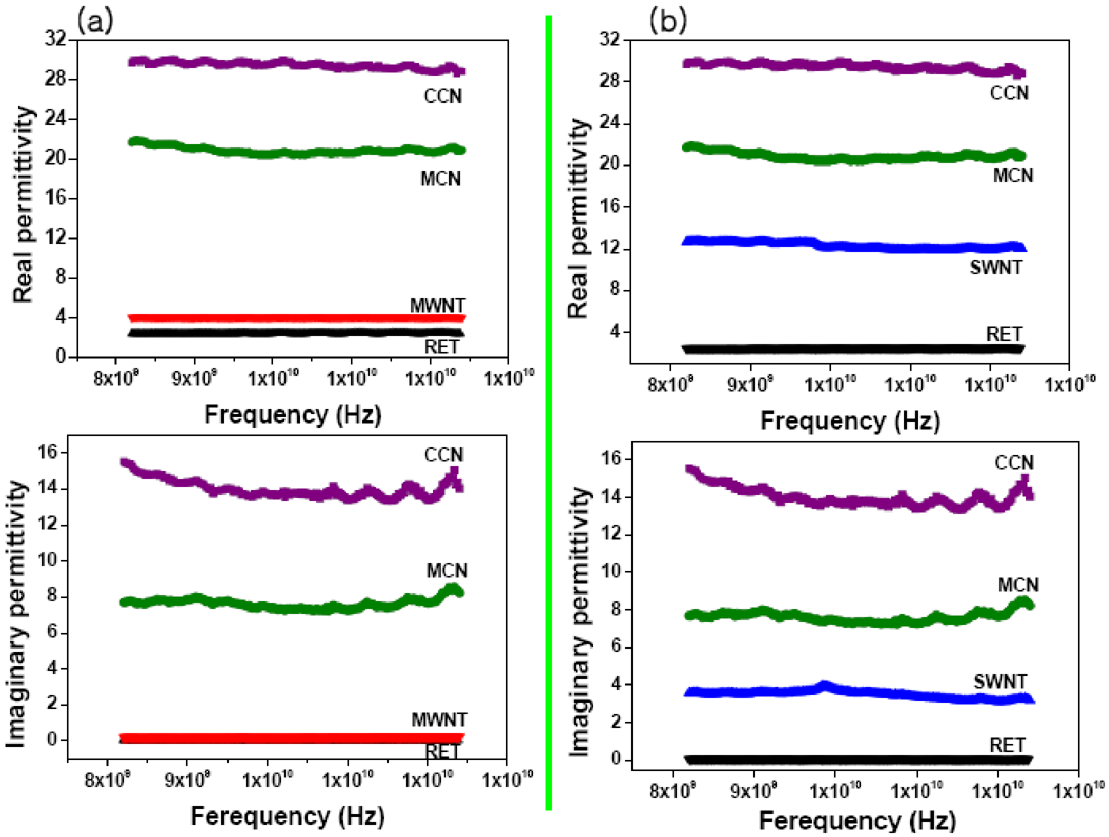

Figure 5-3 Real (top) and imaginary (bottom) permittivity of nanotube composites (Filler: MWNT, SWNT, MCN, CCN) (a) Comparison with similar diameter and length. (b) Comparison with similar DC conductivity.

Based on Figure 5-3, the σ_{AC} (= $2\pi f \varepsilon_0 \varepsilon''$) variation with frequency for the nanocomposites is plotted in Figure 5-4. It was observed that the coiled CNT structure based composite had a higher σ_{AC} compared to the linear SWCNT based composites and the mix (constituted of 50% SWCNTs and 50% coiled CNTs) CNT based composites.

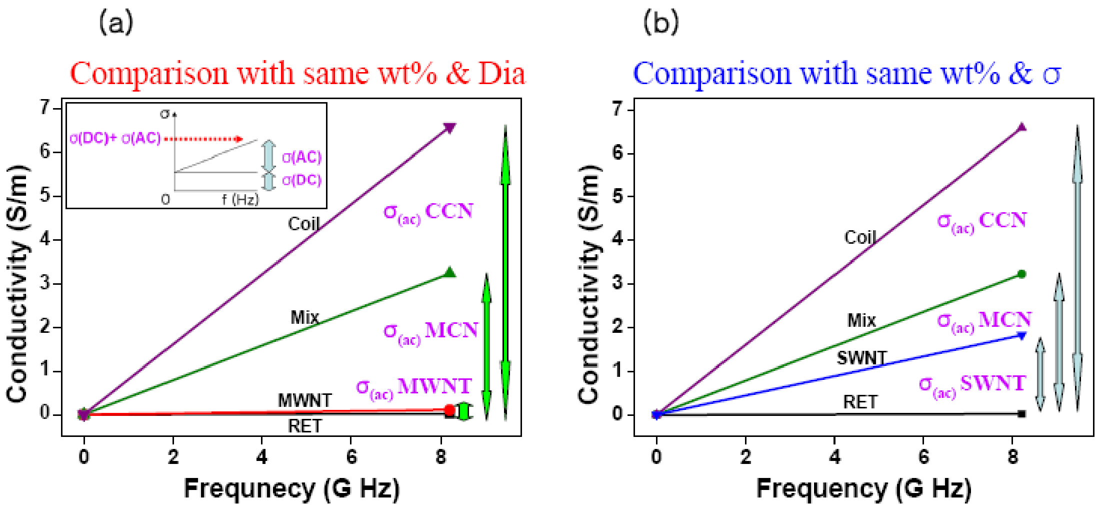

Figure 5-4 The σ_{AC} of nanotube composites at 8.2 G Hz (Filler: MWNT, SWNT, MCN, CCN). (a) Comparison with similar diameter and length. (b) Comparison with similar σ_{DC}. Inset image schematically shows σ_{DC} portion and σ_{AC} portion. Arrow indicates each σ_{AC}. Conductivity at 0 Hz means DC conductivity which is much smaller than AC conductivity.

The larger values of σ_{AC} in the coiled case are explained as due to the larger capacitance, between the turns of the coil - see Figure 5-5, which has the effect of decreasing the capacitive impedance, $X_c \left(= \frac{1}{\omega C}\right)$ and consequently enhancing σ_{AC}.

Concomitantly, a higher EMI SE was also observed for the coiled nanocomposite - Figure 5-6(a) shows a comparison of the SE of CNTs with similar diameters. Figure 5-6(b) shows a comparison of the SE values of samples with similar σ_{DC}. It is also seen from this figure that the SE is much larger for nanocomposites constituted of functionalized SWCNTs compared to those with functionalized

MWCNTs. In all cases, the SE decreases with frequency and corresponds to a reflection dominated mode of EMI shielding[104] and fitted to a $\log_{10}(\frac{\sigma}{f})$ dependence.

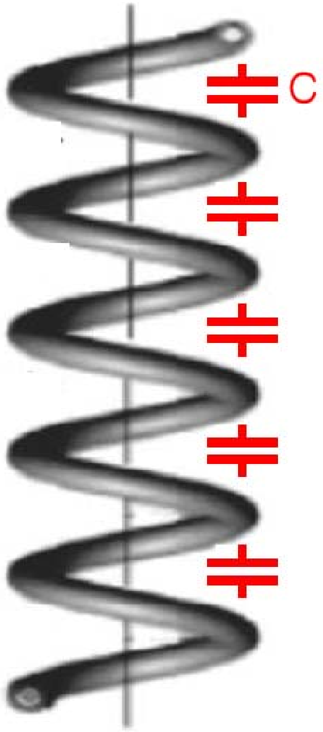

Figure 5-5 Schematic diagram of additional capacitive effect in CCNs

We explain much of the observed dependencies by invoking the length/diameter aspect ratio (A.R.) of the constituent nanostructures (A.R after sonication processes: MWNT ~ 400, SWNT ~ 880, MCN ~1200 and CCN ~ 1700).

We have seen through an elementary application of excluded volume percolation theory[82, 111] that the electrical percolation threshold (ϕ_{perc}) varies inversely with the A.R.- Figure 1-10.

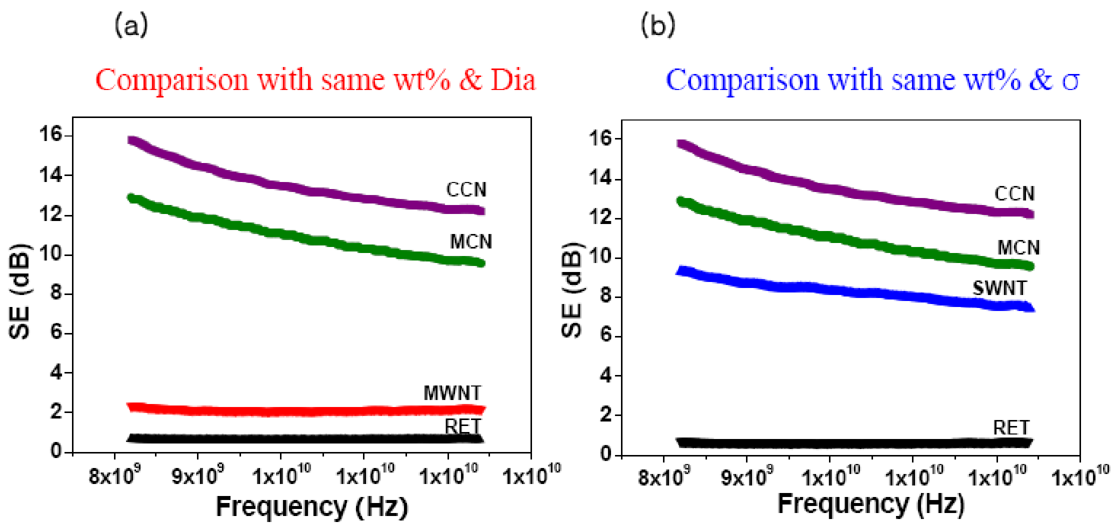

Figure 5-6 Shielding effectiveness (SE) of nanotube composites (Filler: MWNT, SWNT, MCN, CCN) (a) Comparison with similar diameter and length. (b) Comparison with similar DC conductivity.

Consequently, a larger A.R., as in the case of the coiled CNTs, i.e., for the extended coil length would translate to a lower ϕ_{perc}. At a given volume %, above ϕ_c, a higher degree of percolation and enhanced EMI SE is then implied. In our model, it is implied that the entire length of the nanostructure participates in the EMI shielding. Comparing SWCNT and MWCNT constituted nanocomposites, a thirty-fold increase in the A.R. could account for the enhanced SE in the former case. We then propose that the SE could be directly proportional to the A.R. The SE values also seem to follow approximately the rule of mixtures[110], i.e., the SE of the nanocomposite (SE_c) with i constituents could be predicted through $SE_c = \sum_i SE_i \phi_i$, where SE_i refers to the i^{th} constituent. A good agreement (± 10%) with the experimental values was obtained for SE_c.

5.4 Summary

We have seen through a comparison of the electromagnetic properties of polymer nanocomposites constituted of linear and coiled carbon nanotubes, that the EMI shielding efficiency (SE) and dielectric properties are much enhanced in the latter. A higher σ_{AC} (along with ε'') was also recorded through the use helical CNTs, presumably due to enhanced capacitive effects. We explained our experimental observations on the basis of proportionality between the SE and the extended length/diameter aspect ratio of the CNTs. Future work would focus on putting our proposed models on a firm quantitative basis.

Chapter 6. Summary of dissertation

In this dissertation, a detailed study of electrical, electromagnetic and structural characteristics of carbon nanotube-polymer nanocomposites was accomplished.

In the study of EMI shielding properties of CNT composites, nanotube (SWNT/MWNT)-polymer (e.g., RET) system which utilizes functional group interactions for achieving uniform dispersion has low electrical percolation concentrations and enhanced microwave shielding effectiveness. Analysis of the total observed EMI shielding was used for investigating the mechanisms of absorption and reflection in the composite, where a cross-over from reflection dominated shielding to absorption dominated shielding was observed at a CNT volume fraction of ~ 2.3%. It was also concluded that SWNTs were much more effective for shielding, compared to MWNTs. Our proposed scheme of using functionalized CNT-polymer composites together with our obtained results could be used as a basis for light-weight, high shielding efficiency materials for EMI applications.

In the study of dielectric properties of CNT composites, we have seen that functionalized SWNTs, with a high aspect ratio, favor uniform dispersion into an RET polymer matrix and have a major influence on the dielectric properties. We observed a frequency dependent mechanism of electrical conduction of nanotube composites. The relationship of ε'' to σ_{AC} was used as a metric for the EMI shielding effectiveness and understood in terms of a parallel resistor-capacitor model. As the SWNT concentration in the matrix increases, equivalent to an increasing number of parallel resistors and capacitors, the net resistance and capacitive impedance decreases due to the availability of several alternative electrical conduction paths. Future work would focus on the validity of the model and the utility of uniformly dispersed composites for various applications.

In the study of mechanical properties of CNT composites, the interfacial bonding and load transfer is enhanced and enables enhancement in the *E* and *UTS* compared to when unfunctionalized SWNTs are used for filler material. We have also seen that a larger aspect ratio is imperative in enhancing the strength, through comparison with functionalized MWNT reinforced composites. A toughness maximum is indicated at low nanotube volume fractions, mainly caused through incipient crack bridging by the CNTs. However, the toughness is diminished at increased CNT loading due to mechanical percolation effects. Future work would focus on further understanding such effects *vis-a-vis* SWNT volume fraction. It should also be possible to introduce defects at various locations, other than the ends to further improve the toughness.

In the study of dielectric properties and EMI SE properties of nanocoil composites, we have seen through a comparison of the electromagnetic properties of polymer nanocomposites constituted of linear and coiled carbon nanotubes, that the EMI shielding efficiency (SE) and dielectric properties are much enhanced in the latter. A higher σ_{AC} (along with ε'') was also recorded through the use helical CNTs, presumably due to enhanced capacitive effects. We explained our experimental observations on the basis of proportionality between the SE and the extended length/diameter aspect ratio of the CNTs. Future work would focus on putting our proposed models on a firm quantitative basis.

References

[1] S. V. Glushanin, V. Y. Topolov, Krivoruchko AV. Features of piezoelectric properties of 0–3 PbTiO3-type ceramic/polymer composites Materials Chemistry and Physics. 2006;97:357-64.

[2] A. Pelaiz-Barranco, Marin-Franch P. Piezo-, pyro-, ferro-, and dielectric properties of ceramic/polymer composites obtained from two modifications of lead titanate. J Appl Phys. 2005;97:034104.

[3] Z-M. Huang, Y. Z. Zhang, M. Kotakic, Ramakrishnab S. A review on polymer nanofibers by electrospinning and their applications in nanocomposites Compos Sci & Tech. 2003;63:2223-53.

[4] J. Jordan, K. I. Jacob, R. Tannenbaum, M. A. Sharaf, Jasiuk I. Experimental trends in polymer nanocomposites—a review Mat Sci & Eng A. 2005;393:1-11.

[5] Olek M. Carbon nanotube composites mechanical, electrical and optical properties. 2007;Dissertation(University of Bonn).

[6] Chung DDL. Electromagnetic interference shielding effectiveness of carbon materials. Carbon. 2001;39:279.

[7] L. Ci, J. Suhr, V. Pushparaj, X. Zhang, Ajayan PM. Continuous Carbon Nanotube Reinforced Composites. Nano Lett. 2008;8:2762–6.

[8] Bigg DM, Stutz DE. Plastic composites for electromagnetic interference shielding applications. Polymer Composites. 1983;4:40-6.

[9] Rashid ESA, Ariffin K, Akil HM, Kooi CC. Mechanical and Thermal Properties of Polymer Composites for Electronic Packaging Application. Journal of Reinforced Plastics and Composites. 2008;27:1573-84.

[10] Z. Liu, G. Bai, Y. Huang, F. Li, Y. Ma, T. Guo, et al. Microwave Absorption of Single-Walled Carbon Nanotubes/Soluble Cross-Linked Polyurethane Composites. J Phys Chem. 2007;111:13696.

[11] Hughes M. Carbon Nanotube-Conducting Polymer Composites in Supercapacitors. *Dekker Encyclopedia of Nanoscience and Nanotechnology*. London: Taylor & Francis 2004:447-59.

[12] X. Fu, Chung DDL. Submicron-diameter-carbon-filament cement-matrix composites Carbon. 1998;36:459.

[13] Lln JC. Cataracts and cell-phone radiation. IEEE Antennas. 2003;45:171.

[14] P. B. Jana, A. K. Mallick, De SK. Electromagnetic interference shielding by carbon fibre filled polychloroprene rubber composites. Composites. 1991;22:451.

[15] Bigg DM. Mechanical properties of particulate filled polymers. Polym Compos. 1987;8:115.

[16] Bigg DM. Plastic composites for electromagnetic interference shielding applications. Polym Compos. 1983;4:40.

[17] S. Wen, Chung DDL. Partial replacement of carbon fiber by carbon black in multifunctional cement–matrix composites. Carbon. 2007;45:505.

[18] Chung DDL. Electrically conductive cement-based materials. Adv Cem Res. 2004;16:167.

[19] B. O. Lee, W. J. Woo, Kim MS. EMI Shielding Effectiveness of Carbon Nanofiber Filled Poly(vinyl alcohol) Coating Materials. Macromol Mater Eng. 2001;286:114.

[20] Y. J. Chen, M. S. Cao, T. H. Wang, Wan Q. Microwave absorption properties of the ZnO nanowire-polyester composites. Appl Phys Lett. 2004;84:3367.

[21] Y. Yang, M. C. Gupta, K. L. Dudley, Lawrence RW. Novel Carbon Nanotube-Polystyrene Foam Composites for Electromagnetic Interference Shielding. Nano Lett. 2005;5:2131.

[22] N. Li, Y. Huang FD, X. He, X. Lin, H. Gao, Y. Ma, et al. Electromagnetic Interference (EMI) Shielding of Single-Walled Carbon Nanotube Epoxy Composites. Nano Lett. 2006;6:1141.

[23] Oberlin A, Endo M, Koyama T. Filamentous growth of carbon through benzene decomposition J Cryst Growth 1976;32:335 – 49.

[24] R. H. Baughman, A. A. Zakhidov, Heer WAd. Carbon Nanotubes--the Route Toward Applications Science. 2002;297:787.

[25] Popov VN. Carbon nanotubes: properties and application Mater Sci Eng. 2004;43:61.

[26] A. Wadhawan, D. Garrett, Perez JM. Nanoparticle-assisted microwave absorption by single-wall carbon nanotubes. Appl Phys Lett. 2003;83:2683.

[27] K. Balasubramanian MB. Chemically Functionalized Carbon Nanotubes. Small. 2005;1:180.

[28] Iijima S. Helical microtubules of graphite carbon. Nature 1991;354:56-8.

[29] Y. L Yang, M. C. Gupta, K. L. Dudley, Lawrence RW. Conductive Carbon Nanofiber-Polymer Foam Structures. Adv Mater. 2005;17:1999.

[30] M. Zhang, S. L. Fang, A. A. Zakhidov, S. B. Lee, A. E. Aliev, C. D. Williams, et al. Strong, Transparent, Multifunctional, Carbon Nanotube Sheets Science. 2005;309:1215.

[31] A. Peigney, C. Laurent, E. Flahaut, R. R. Bacsa, Rousset A. Specific surface area of carbon nanotubes and bundles of carbon nanotubes. Carbon. 2001;39:507-14.

[32] Images from Hanwha Nanotech Corporation, (www.hanwhananotech.com), Schematic images of carbon nanotubes.

[33] C. A. Dyke, Tour JM. Covalent Functionalization of Single-Walled Carbon Nanotubes for Materials Applications. Phys Chem A. 2004;108:11151.

[34] J. L. Bahr, E. T. Mickelson, M. J. Bronikowski, R. E. Smalley, Tour JM. Dissolution of small diameter single-wall carbon nanotubes in organic solvents? Chem Commun. 2001;2:193.

[35] M. Moniruzzaman, Winey KI. Polymer Nanocomposites Containing Carbon Nanotubes Macromolecules. 2006;39:5194.

[36] D. Tasis, N. Tagmatarchis, A. Bianco, Prato M. Chemistry of Carbon Nanotubes. Chem Rev. 2006;106:1105-36.

[37] J. Chen, M. A. Hamon, H. Hu, Y. S. Chen, A. M. Rao, P. C. Eklund, et al. Solution Properties of Single-Walled Carbon Nanotubes. Science. 1998;282:95.

[38] Y. Sun, W. Huang, Carroll DL. Soluble dendron-functionalized carbon nanotubes: preparation, characterization and properties. Chem Matter. 2001;13:2864.

[39] Y. Lin, M. J. Meziani, Sun YP. Functionalized carbon nanotubes for polymeric nanocomposites. J Mat Chem. 2007;17:1143.

[40] H. Hu, P. Bhowmik, B. Zhao, M. A. Hamon, M. E. Itkis, Haddon RC. Determination of the acidic sites of purified single-walled carbon nanotubes by acid–base titration. Chem Phys Lett, 2001, 345,25. 2001;345:25.

[41] J. Gao, B. Zhao, M. E Itkis, E. Bekyarova, H. Hu, V. Kranak, et al. Chemical Engineering of the Single-Walled Carbon Nanotube−Nylon 6 Interface. J Am Chem Soc. 2006;128:7492.

[42] A. Star, Y. Liu, K. Grant, L. Ridvan, J. F. Stoddart, D. W. Steuerman, et al. Noncovalent Side-Wall Functionalization of Single-Walled Carbon Nanotubes. Macromolecules. 2003;36:553-60.

[43] A. Saib, L. Bednarz, R. Daussin, C. Bailly, X. Lou, J. M. Thomassin, et al. Carbon Nanotube Composites for Broadband Microwave Absorbing Materials. IEEE Trans. 2006;54:2745.

[44] Deutscher G. In percolation and superconductivity. edited by A M Goldman and S A Wolf (plenum, New York, 1984).109:95.

[45] C.J. Lobb, Frank DJ. A large-cell renormalisation group calculation of the percolation conduction critical exponent. J Phys. 1979;12:827.

[46] B. E. Kilbride, J. N. Coleman, J. Fraysse, P. Fournet, M. Cadek, A. Drury, et al. Experimental observation of scaling laws for alternating current and direct current conductivity in polymer-carbon nanotube composite thin films. J Appl Phys. 2002;92:4024.

[47] F. Du, R. C. Scogna, W. Zhou, S. Brand, J. E. Fischer, Winey KI. Nanotube Networks in Polymer Nanocomposites: Rheology and Electrical Conductivity. Macromolecules. 2004;37:9048.

[48] V. Skákalová, U. Dettlaff-Weglikowska, Roth S. Electrical and mechanical properties of nanocomposites of single wall carbon nanotubes with PMMA. Synthetic Metals. 2005;152:349.

[49] E. Kymakis, Amaratunga GAJ. Electrical properties of single-wall carbon nanotube-polymer composite films. J Appl Phys. 2006;99:084302.

[50] B. Kim, J. Lee, Yu I. Electrical properties of single-wall carbon nanotube and epoxy composites. J Appl Phys. 2003;94:6724.

[51] P. Potschke, Dudkin SM. Dielectric spectroscopy on melt processed polycarbonate—multiwalled carbon nanotube composites Polymer. 2003;44:5023.

[52] G. J. Hu, C. G. Zhao, S. M. Zhang, M. S. Yang, Wang ZG. Low percolation thresholds of electrical conductivity and rheology in poly(ethylene terephthalate) through the networks of multi-walled carbon nanotubes Polymer. 2006;47:480.

[53] Z. Fan, G. Luo, Z. Zhang, L. Zhou, Wei F. Electromagnetic and microwave absorbing properties of multi-walled carbon nanotubes/polymer composites. Mats Sci & Eng B. 2006;132:85-9.

[54] G. E. Pike, Seager CH. Percolation and conductivity: A computer study. Phys Rev B. 1974;10:1421.

[55] N. Ueda, Taya M. Proc ICCM-V, AIME, Harigan, WC,. 1985:1727.

[56] N. Ueda, Taya M. Prediction of the electrical conductivity of two-dimensionally misoriented short fiber composites by a percolation model. J Appl Phys. 1986;60:459.

[57] N. Ueda, Taya M. J Eng Mat & Tech. 1987;109:225.

[58] I Balberg, C. H. Anderson, S. Alexander, Wagner N. Excluded volume and its relation to the onset of percolation. Phys Rev B. 1984;30:3933-43.

[59] I. Balberg, Binenbaum N. Cluster structure and conductivity of three-dimensional continuum systems. Phys Rev A. 1985;31:1222.

[60] Balberg I. Excluded-volume explanation of Archie's law. Phys Rev B. 1986;33:3618.

[61] S. Wu, I. Masaharu, T. Natsuki, Ni Q. Electrical conduction and percolatioin behavior of carbon nanotube/UPR nanocomposites. Journal of Reinforced plastic and Composite. 2006;25:1957-66.

[62] Onsager L. The effects of shape on the interaction of colloidal particles. Ann NY Acad Sci. 1949;51:627.

[63] I. Balberg, Binenbaum N. Computer study of the percolation threshold in a two-dimensional anisotropic system of conducting sticks. Phys Rev B. 1983;28:3799.

[64] S. W. Haan, Zwanzig R. Series expansions in a continuum percolation problem. J phys A. 1977;10:1547.

[65] B. Safadi, R. Andrews, Grulke EA. Multiwalled carbon nanotube polymer composites: Synthesis and characterization of thin films. J Appl Polymer Science. 2002;84:2660.

[66] D. Qian, E. C. Dickey, R. Andrews, Rantell T. Load transfer and deformation mechanisms in carbon nanotube-polystyrene composites. Appl Phys Lett. 2000;76:2868.

[67] M. Moniruzzaman, J. Chattopadhyay, W. E. Billups, Winey KI. Tuning the mechanical properties of SWNT/Nylon 6,10 composites with flexible spacers at the interface. Nano Lett. 2007;7:1178-85.

[68] J. M. Benoit, B. Corraze, S. Lefrant, W. J. Blau, Bernier P. Transport properties of PMMA-Carbon Nanotubes composites Synth Met. 2001;121:1215.

[69] F. Du JEF, K. Winey. Coagulation method for preparing single-walled carbon nanotube/poly(methyl methacrylate) composites and their modulus, electrical conductivity, and thermal stability. J Polym Phys. 2003;41:3333.

[70] M. L. Shofner, V. N. Khabashesku, Barrera EV. Processing and Mechanical Properties of Fluorinated Single Wall Carbon Nanotube-Polyethylene Composites. Chemistry of Materials. 2006;18:906.

[71] Q. H. Zhang, S. Rastogi, D. J. Chen, D. Lippits, Lemstra PJ. Low percolation threshold in single-walled carbon nanotube/high density polyethylene composites prepared by melt processing technique Carbon 2006;44:778.

[72] W. D. Zhang, L. Shen, I. Y. Phang, Liu T. Carbon Nanotubes Reinforced Nylon-6 Composite Prepared by Simple Melt-Compounding. Macromolecules 2004;37:256.

[73] T. D. Fornes, J. W. Baur, Y. Sabba, Thomas EL. Morphology and properties of melt-spun polycarbonate fibers containing single- and multi-wall carbon nanotubes Polymer. 2006;47:1704.

[74] A. R. Bhattacharyya, T. V. Sreekumar, Liu T. Crystallization and orientation studies in polypropylene/single wall carbon nanotube composite Polymer 2003;44:2373.

[75] E. J. Siochi, D. C. Working, C. Park, Kumar S. Melt processing of SWCNT-polyimide nanocomposite fibers Composites, Part B. 2004;35B:439.

[76] J. Zhu, J. Kim, H. Peng, J. L. Margrave, V. N. Khabashesku, Barrera EV. Improving the Dispersion and Integration of Single-Walled Carbon Nanotubes in Epoxy Composites through Functionalization. Nano Lett. 2003;3:1107-13.

[77] J. Zhu, H. Peng, F. Rodriguez-Macias, J. L. Margrave, V. N. Khabashesku, A. M. Imam, et al. Reinforcing Epoxy Polymer Composites Through Covalent Integration of Functionalized Nanotubes. AdV Funct Mater. 2004;14:643.

[78] Breuer O, Sundararaj U. Big returns from small fibers: A review of polymer/carbon nanotube composites. Polymer Composites. 2004;25:630-45.

[79] Ott HW. Noise reduction techniques in electronic systems. New York: John Wiley & Sons 1988.

[80] Wang Y, Jing X. Intrinsically conducting polymers for electromagnetic interference shielding. Polymers for Advanced Technologies. 2005;16:344-51.

[81] Chung DDL. Electromagnetic Interference Shielding Effectiveness of Carbon Materials. Carbon. 2001;39:279-85.

[82] Balberg I, Anderson CH, Alexander S, Wagner N. Excluded volume and its relation to the onset of percolation. Physical Review B. 1984;30:3933-43.

[83] Celzard A, McRae E, Deleuze C, Dufort M, Furdin G, Mareche JF. Critical concentration in percolating systems containing a high-aspect ratio filler. Physical Review B. 1996;53:6209-14.

[84] Li N, Huang Y, Du F, He X, Lin X, Gao H, et al. Electromagnetic Interference (EMI) Shielding of Single-Walled Carbon Nanotube Epoxy Composites. Nanoletters. 2006;6:1141-5.

[85] Huang Y, Li N, Ma Y, Du F, Li F, He X, et al. The influence of single-walled carbon nanotube structure on the electromagnetic interference shielding efficiency of its epoxy composites. Carbon. 2007;45:1614-21.

[86] Liu Z, Bai G, Huang Y, Ma Y, Du F, Li F, et al. Reflection and absorption contributions to the electromagnetic interference shielding of single-walled carbon nanotube/polyurethane composites. Carbon. 2007;45:821-7.

[87] Das NC, Maiti S. Electromagnetic interference shielding of carbon nanotube/ethylene vinyl acetate composites. J Mater Sci. 2008;43:1920-5.

[88] Xu H, Anlage SM, Hu L, Gruner G. Microwave shielding of transparent and conducting single-walled carbon nanotube films. Appl Phys Lett. 2007;90:183119.

[89] Tasis D, Tagmatarchis N, Bianco A, Prato M. Chemistry of Carbon Nanotubes. Chemical Reviews. 2006;106:1105-35.

[90] Antoniotti S, Antonczak S, Golebiowski J. Acid-catalyzed oxidative ring-opening of epoxide by DMSO. Theoretical investigation of the effect of acid catalysts and substituents. Theoretical Chemistry Accounts. 2004;112:290-7.

[91] Bekyarova E, Thostenson ET, Yu A, Itkis ME, Fakhrutdinov D, Chou T-W, et al. Functionalized single-walled carbon nanotubes for carbon fiber-epoxy composites. Journal of Physical Chemistry C. 2007;111:17865-71.

[92] Nichols JA, Saito H, Deck C, Bandaru PR. Artificial introduction of defects into vertically aligned multiwall carbon nanotube ensembles: Application to electrochemical sensors. Journal of Appled Physics. 2007;102:064306.

[93] Lin Y, Meziani MJ, Sun Y-P. Functionalized carbon nanotubes for polymeric nanocomposites. J Mater Chem. 2007;17:1143-8.

[94] Haggenmueller R, Fischer JE, Winey KI. Single wall carbon nanotube/polyethylene nanocompoites: Nucleating and templating polyethylene crystallites. Macromolecules. 2006;39:2964-71.

[95] Bryning MB, Islam MF, Kikkawa JM, Yodh AG. Very low conductivity threshold in bulk isotropic single-walled carbon nanotube-epoxy composites. Advanced Materials. 2005;17:1186-91.

[96] Fan Z, Luo G, Zhang Z, Zhou L, Wei F. Electromagnetic and microwave absorbing properties of multi-walled carbon nanotubes/polymer composites. Mater Sci Eng, B. 2006;132:85-9.

[97] Moniruzzaman M, Winey KI. Polymer nanocomposites containing carbon nanotubes. Macromolecules. 2006;39:5194-205.

[98] Pozar DM. Microwave Engineering. 2 ed. New York: John Wiley & Sons, Inc. 1998.

[99] Engen GF, Hoer CA. "Thru-Reflect-Line" : An Improved Technique for Calibrating the Dual Six-Port Automatic Network Analyzer IEEE Transactions Microave Theory and Techniques. 1979;MTT-27:987-93.

[100] Wilson PF, Ma MT, Adams JW. Techniques for measuring the electromagnetic shieldingeffectiveness of materials. I. Far-field source simulation. IEEE Transactions on Electromagnetic Compatibility. 1988;30:239-50.

[101] McLachlan DS, Blaszkiewicz M, Newnham RE. Electrical Resistivity of Composites. J Am Ceram Soc. 2005;73:2187-203.

[102] Saib A, Bednarz L, Daussin R, Bailly C, Lou X, Thomassin JM, et al. Carbon nanotube composites for broadband microwave absorbing materials. IEEE Transactions on Microwave Theory and Techniques. 2006;54:2745-54.

[103] Kim HM, Kim K, Lee CY, Joo J, Cho SJ, Yoon HS, et al. Electrical conductivity and electromagnetic interference shielding of multiwalled carbon nanotube composites containing Fe catalyst. Appl Phys Lett. 2004;84:589-91.

[104] Sengupta DL, Liepa VV. Applied Electromagnetics and Electromagnetic Compatibility. New York: John Wiley & Sons, Inc. 2005.

[105] Ajayan P, Schadler LS, Giannaris C, Rubio A. Single-Walled Carbon Nanotube-Polymer Composites: Strength and Weakness. Advanced Materials. 2000;12:750-3.

[106] H. Xu, S. M. Anlage, L. Hu, Gruner G. Microwave shielding of transparent and conducting single-walled carbon nanotube films. Appl Phys Lett. 2007;90:183119-3.

[107] Z. Liu, G. Bai, Y. Huang, Y. Ma, F. Du, F. Li, et al. Reflection and absorption contributions to the electromagnetic interference shielding of single-walled carbon nanotube/polyurethane composites. Carbon. 2007;45:821.

[108] Nicolson AM, Ross GF. Measurement of the intrinsic properties of materials by time-domain techniques. IEEE Transactions on Instrumentation and Measurement. 1970;1M-19:377-82.

[109] Weir WB. Automatic measurement of complex dielectric constant and permeability at microwave frequencies. Proceedings of the IEEE. 1974;62:33-6.

[110] Todd MG, Shi FG. Complex permittivity of composite systems: a comprehensive interphase approach. IEEE Transactions on Dielectrics and Electrical Insulation. 2005;12:601-11.

[111] Kirkpatrick S. Percolation and conduction. Reviews of Modern Physics. 1973;45:574-88.

[112] Al-Saleh M, Sundararaj U. Electromagnetic interference (EMI) shielding effectiveness of PP/PS polymer blends containing high structure carbon black Macromolecular Materials and Engineering. 2008;293:621-30.

[113] Halpin JC, Kardos JL. The Halpin-Tsai equations: A Review. Polym Eng Sci. 1976;16:344-52.

[114] Peigney A, Laurent C, Flahaut E, Basca RR, Rousset A. Specific surface area of carbon nanotubes and bundles of carbon nanotubes. Carbon. 2001;39:507-14.

[115] Ni C, Chattopadhyay J, Billups WE, Bandaru PR. Modification of the electrical characteristics of single wall carbon nanotubes through selective functionalization. Appl Phys Lett. 2008;93:243113.

[116] K. H. Kim, Jo WH. A strategy for enhancement of mechanical and electrical properties of polycarbonate/multi-walled carbon nanotube composites. Carbon. 2009;47:1126-34.

[117] M. K. Yeh, N. H. Tai, Liu JH. Mechanical behavior of phenolic-based composites reinforced with multi-walled carbon nanotubes. Carbon. 2006;44:1-9.

[118] M. K. Yeh, N. H. Tai, Lin YJ. Mechanical properties of phenolic-based nanocomposites reinforced by multi-walled carbon nanotubes and carbon fibers. Composites, Part A. 2008;39:677-84.

[119] M.A. Lo´pez Manchado, L. Valentini, J. Biagiotti, Kenny JM. Thermal and mechanical properties of single-walled carbon nanotubes–polypropylene composites prepared by melt processing. Carbon. 2005;43:1499-505.

[120] N. H. Tai, M. K. Yeh, Peng TH. Experimental study and theoretical analysis on the mechanical properties of SWNTs/phenolic composites. Composites B. 2008;39:926-32.

[121] J. Gao, M. E. Itkis, A. Yu, E. Bekyarova, B. Zhao, Haddon RC. Continuous Spinning of a Single-Walled Carbon Nanotube−Nylon Composite Fiber. J Am Chem Soc. 2005;127:3847-54.

[122] M. C. Paiva, B. Zhou, K. A. S. Fernando, Y. Lin, J. M. Kennedy, Sun YP. Mechanical and morphological characterization of polymer–carbon nanocomposites from functionalized carbon nanotubes. Carbon. 2004;42:2849-54.

[123] L. Sun, G. L. Warren, J. Y. O'Reilly, W. N. Everett, S. M. Lee, D. Davis, et al. Mechanical properties of surface-functionalized SWCNT/epoxy composites. Carbon. 2008;46:320-28.

[124] C. T. Love, Karbhari VM. Filled reactive ethylene terpolymer primers for cathodic disbondment mitigation. J Appl Pol Sci. 2008;110:1531-44.

[125] J. C. Halpin, Tsai SW. Effects of environmental factors on composite materials. Technical Report AFML-TR-67-423. 1969.

[126] A. Kis, G. Csányi, J. P. Salvetat, T. N. Lee, E. Couteau, A. J. Kulik, et al. Reinforcement of single-walled carbon nanotube bundles by intertube bridging. Nature Mat. 2004;3:153-7.

[127] D. Qian, E. C. Dickey, R. Andrews, Rantell T. Load transfer and deformation mechanisms in carbon nanotube-polystyrene composites. Appl Phys Lett. 2000;76:2868-70.

[128] F. H. Gojny, M. H. G. Wichmann, U. Kopke, B. Fiedler, Schulte K. Carbon nanotube-reinforced epoxy-composites: enhanced stiffness and fracture toughness at low nanotube content. Compos Sci & Tech. 2004;64:2363-71.

[129] P. M. Ajayan, L. S. Schadler, C. Giannaris, Rubio A. Single-Walled Carbon Nanotube-Polymer Composites: Strength and Weakness. Adv Mater. 2000;12:750-3.

[130] Balasubramanian K, Burghard M. Chemically Functionalized Carbon Nanotubes. Small. 2005;2:180-92.

[131] F. H. Gojny, M. H. G. Wichmann, B. Fiedler, Schulte K. Influence of different carbon nanotubes on the mechanical properties of epoxy matrix composites – A comparative study Compos Sci & Tech. 2005;65:2300-13.

[132] S. H. Park, P. Thielemann, P. Asbeck, Bandaru P. Enhanced dielectric constants and shielding effectiveness of, uniformly dispersed, functionalized carbon nanotube composites. Appl Phys Lett. 2009;94:243111-3.

[133] S. H. Park, P. Telemann, P. Asbeck, Bandaru PR. Enhanced electromagnetic interference shielding through the use of functionalized carbon nanotube-reactive polymer composites IEEE Transactions on Nanotechnology. 2009;Submitted.

[134] E. Bekyarova, E. T. Thostenson, A. Yu MEI, D. Fakhrutdinov, T. W. Chou, Haddon RC. Functionalized Single-Walled Carbon Nanotubes for Carbon Fiber-Epoxy Composites. J Phys Chem C. 2007;111:17865-71.

[135] Nichols J, Deck CP, Saito H, Bandaru PR. Artificial introduction of defects into vertically aligned multiwalled carbon nanotube ensembles: Application to electrochemical sensors. J Appl Phys. 2007;102:064306.

[136] Wang W, Yang K, Gaillard J, Bandaru PR, Rao AM. Rational synthesis of helically coiled carbon nanowires and nanotubes through the use of Tin and Indium catalysts. Advanced Materials. 2008;20:179-82.

[137] Bandaru PR. Electrical Properties and Applications of Carbon Nanotube Structures. Journal of Nanoscience and Nanotechnology. 2007;7:1239-67.

[138] Daraio C, Jin S, Nesterenko V, Wang W, Rao AM. Impact Response by a Foamlike Forest of Coiled Carbon Nanotubes. Journal of Applied Physics. 2006;100:064309.

[139] Chen X, Zhang S, Dikin DA, Ding W, Ruoff RS, Pan L, et al. Mechanics of a carbon nanocoil. Nanoletters. 2003;3:1299-304.

[140] Bandaru PR, Daraio C, Yang K, Rao AM. A plausible mechanism for the evolution of helical forms in nanostructure growth. J Appl Phys. 2007;101: 094307.